PHYSICAL REVIEW A VOLUME 8, NUMBER 1 JULY 1983

Statistical mechanics of neocortical interactions. Dynamics of synaptic modification

Lester Ingber
Physical Studies Institute, Drawer W, Solana Beach, California 92075
and Institute of Pure and Applied Physical Sciences, University of California, San Diego, La Jolla, California 92093
(Received 30 August 1982)

A recent study has demonstrated that several scales of neocortical interactions can be consistently analyzed with the use of methods of modern nonlinear nonequilibrium statistical mechanics. The formation, stability, and interaction of spatial-temporal patterns of columnar firings are explicitly calculated, to test hypothesized mechanisms relating to information processing. In this context, most probable patterns of columnar firings are associated with chemical and electrical synaptic modifications. It is stressed that synaptic modifications and shifts in most-probable firing patterns are highly nonlinear and interactive sets of phenomena. A detailed scenario of information processing is calculated of columnar coding of external stimuli, short-term storage via hysteresis, and long-term storage via synaptic modification.

I. INTRODUCTION

An analytic formulation of neocortical information processing, consistent with and based upon current data, has been developed which is applicable to a broad range of relevant spatial scales, with the use of methods of modern nonlinear nonequilibrium (e.g., evolving irreversibly) statistical mechanics.[1] As referenced in that work, there are many previous studies of cortex that have made severe approximations not found to be necessary here. Perhaps the most important feature of this work is that some aspects of neocortical phenomena now come within the scope of current paradigms of collective systems, expanding the interdisciplinary approach to this complex system.[2–5]

A major contribution of this work is the analytic treatment of minicolumns.[6] Minicolumns are structures observed to span $\sim 7\times 10^2\ \mu m^2$. Mesocolumnar domains are defined here as the spatial extent of minicolumns, in order to distinguish their scale from that of microscopic neurons, but they retain neuronal chemical and electrical properties. The proper stochastic treatment of their interaction permits their development into macroscopic regions responsible for global neocortical information processing.

The basic hypothesis is that neocortical development and function can be correctly represented by specific microscopic circuitries, upon which is superimposed a set of short-ranged interactions constrained by a nonlinear nonequilibrium statistical mechanics which guides the more microscopic electrical-chemical biophysics. Furthermore, in the context of global information processing, even the specific microscopic circuitries are subject to further averaging. Support for arguments invoking stochastic processing to explain empirical observations range from electroencephalographic (EEG)[7–9] and magnetoencephalographic (MEG)[10] (having resolution in the range of millimeters) studies to studies of neuronal development and death.[11]

Since neuronal and columnar firings transpire in epochs on the order of milliseconds, and synaptic modifications take place in epochs on the order of tenths to many seconds, modifications must take place in the (nonlinear) environment of changing eigenfunctions, i.e., firing states, of the firing patterns. I.e., it is reasonable to assume that synaptic modifications generally follow changes in firing patterns adiabatically. Linear algebraic approaches are appropriate only after the nonlinear problem has been solved for most probable firing states for a given set of neuronal parameters.

Previous approaches do not consider the evolution of synaptic modifications as transpiring in the context of interacting with changing firing patterns.[1] This is essential since the latter most usually cause the former. In this study these efficacies can be better represented as more specific presynaptic or postsynaptic modifications, and therefore ultimately they permit theory based on them to be more testable. Instead of somewhat nonrigorously examining synaptic modifications of an "average" neuron, this theory relatively rigorously examines the average synaptic modification of a mesocolumn consisting of over a hundred neurons.

Section II outlines the derivation of the statistical

mechanics of firing patterns[1] in the context of this paper, and adds explicit polynomial expansions to detail the ranges where such approximations are useful. More detailed biological, mathematical and physics support and references for this development are given in Ref. 1. However, enough descriptive and mathematical detail are given here to be self-contained, and to at least convey the nature of the nonlinearities and multiple hierarchies inherent in neocortex.

Section III considers the dynamics of synaptic modification, and includes calculations of synaptic coding of extrinsic stimuli and the stability of synaptic modifications. Estimates of the probability of hysteresis are calculated using the development of Sec. II. Initial results are presented of a Monte Carlo program that explicitly calculates the probability distribution of firing patterns. Extensions of this algorithm are described for future study of interlaminar and inter-regional interactions and chaotic behavior.

Thus the statistical mechanics of a detailed scenario is explicitly calculated, of columnar coding of extrinsic stimuli, short-term storage via hysteresis, and long-term storage via synaptic modification. The price paid for using a statistical mechanics paradigm to obtain the conceptual simplicity of these results consists of a relatively long formal development and computer calculations and rather tedious expansions of the derived highly nonlinear functions.

II. STATISTICAL MECHANICS OF FIRING PATTERNS

A. Microscopic neurons

Briefly stated, at the membrane level neuron-neuron interactions proceed at ionic and molecular scales via gates regulated by electrical and chemical activity, by mechanisms currently under biochemical and statistical mechanical investigations[12,13]: Voltage-gated axonal transmembrane ionic flows along a firing efferent neuron, e.g., of Na^+ and K^+ sequentially, propagate an action potential of ~ 100 mV. This acts to voltage-gate presynaptic transmembrane ionic flows, e.g., of Ca^{2+}, causing the release of "quanta" of neurotransmitter, each quanta containing $\sim 10^3$ molecules, e.g., glutamic acid (excitatory) or γ-aminobutyric acid (inhibitory). Molecules of neurotransmitters that survive interactions through the synaptic cleft act to chemically gate postsynaptic transmembrane ionic flows, e.g., of Na^+ and K^+ simultaneously (excitatory) or of K^+ and/or Cl^- (inhibitory), which depolarize or hyperpolarize the postsynaptic membrane. With sufficient depolarization transduced at the trigger site of its axon from its synapses, typically located on dendrites and the cell body (soma), the afferent neuron fires, i.e., initiates an action potential, and becomes efferent to many other neurons via its branching axon and axonal collaterals. Coincidence gating mechanisms, not considered here, can cause specific microscopic circuitries to be sensitive to time scales ~ 0.01 msec.

Calculations[1] demonstrate that the probability of a given neuron firing within a refractory period of $\tau_n \sim 5$ msec because of its neuronal interactions is essentially independent of the functional form, not the numerical mean and variance, of the average interneuronal distribution of chemical quanta. τ_n is taken to lie between an absolute refractory period of ~ 1 msec, during which another action potential cannot be initiated, and a relative refractory period of ~ 0.5—10 msec (larger neurons typically having larger periods), during which a stronger stimulus is required to initiate another action potential. A Gaussian distribution Γ is reasonable to describe the average intraneuronal distribution of electrical polarization across the various shapes and sizes of neurons in a mesocolumn. Throughout this study, excitatory (E) and inhibitory (I) firings retain their chemically mediated independences in neocortex.

Consider the interaction of neuron k ($k=1,N^*$) with neuron j across all jk synapses according to a distribution Ψ for q chemical quanta with mean efficacy $a^*_{jk}=\frac{1}{2}A^*_{jk}(\sigma_k+1)+B^*_{jk}\sim 0.01$, with B^*_{jk} a background spontaneous contribution; $\sigma_k=1$ if k fires; $\sigma_k=-1$ if k does not fire. Synaptic efficacy is a measure of ionic permeability, and an inverse measure of electrical impedance. Efficacies A^*_{jk} measure chemical synaptic activity; efficacies B^*_{jk} measure various small but measurable influences, e.g., local couplings between transient postsynaptic polarizations (electrotonic potentials),[14] remote couplings to transient extracellular fields of action potentials (ephaptic interactions),[15] and fluctuations in extracellular ions especially in the wake of action potentials. As portrayed in Fig. 1, the final electrical effect at the trigger zone of j is described by a Gaussian distribution Γ with mean qv_{jk} and variance $\sqrt{q}\,\phi_{jk}$, with $v_{jk}\sim\phi_{jk}\sim 0.1$ mV. Neuron j fires if the threshold electric potential $V_j\sim 10$ mV is attained at the trigger zone of the axon. Numerical values of these parameters agree with those observed in experimental studies.[16–18] A net effect is to make the firing of neuron j, near its firing threshold within τ_n, sensitive to changes of firing of $\sim 10^{-3}$—$10^{-2}N^*$ of its efferents $\{k\}$. Neuronal firing rates typically are $<0.1/\tau_n$.

[Although recent studies favor a binomial distri-

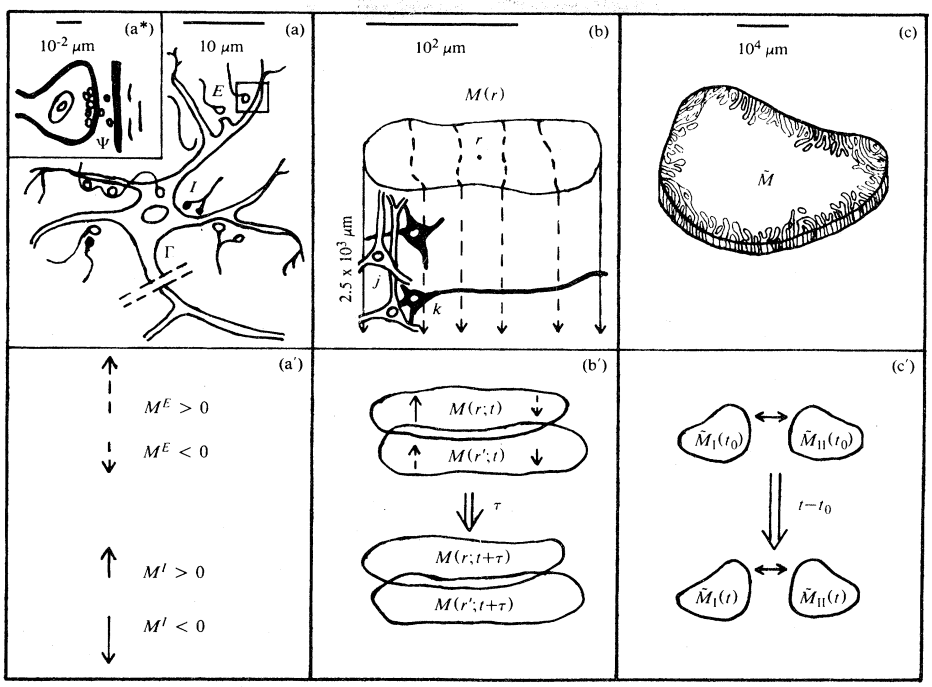

FIG. 1. Illustrated are three biophysical scales of neocortical interactions: (a)-(a*)-(a') microscopic neurons; (b)-(b') mesocolumnar domains; (c)-(c') macroscopic regions. In (a*) synaptic interneuronal interactions, averaged over by mesocolumns, are phenomenologically described by the mean and variance of a distribution Ψ. Similarly, in (a) intraneuronal transmissions are phenomenologically described by the mean and variance of Γ. Mesocolumnar averaged excitatory (E) and inhibitory (I) neuronal firings are represented in (a'). In (b) the vertical organization of minicolumns is sketched together with their horizontal stratification, yielding a physiological entity, the mesocolumn. In (b') the overlap of interacting mesocolumns is sketched. In (c) macroscopic regions of neocortex are depicted as arising from many mesocolumnar domains. These are the regions designated for study here. (c') sketches how regions may be coupled by long-ranged interactions.

bution for Ψ over a Poisson distribution,[17] it should be noted that in that paper, albeit studying goldfish synapses, their variance σ in their L (Γ here) should be replaced by $\sqrt{k}\,\sigma$ ($\sqrt{q}\,\phi_{jk}$ here), which arises from the application of the "central limit theorem"[19] to independent Gaussian processes of q released quanta. That error appears to bias their results for their p_k (Ψ here) towards the binomial distribution, although their final conclusions may not require substantial revision.]

The derived probability for neuron j to fire, given its interaction with $k=1,\ldots,N^*$ neurons is

$$p_{\sigma_j}=\int_{V_j}^{\infty} dW_j S_j \simeq \exp(-\sigma_j F_j)/[\exp F_j+\exp(-F_j)]\,, \tag{2.1}$$

$$F_j=\left[V_j-\sum_k a_{jk}^* v_{jk}\right]\Big/\left[\pi\sum_{k'} a_{jk'}^*(v_{jk'}^2+\phi_{jk'}^2)\right]^{1/2},$$

$$S_j=\int\cdots\int dW_{j1}\cdots dW_{jN^*} S_{j1}\cdots S_{jN^*}\,\delta\left[W_j-\sum_k W_{jk}\right],$$

$$S_{jk}=\sum_{q=0}^{\infty}\Gamma\Psi\,,$$

$$\Gamma=(2\pi q\phi_{jk}^2)^{-1/2}\exp[-(W_{jk}-qv_{jk})^2]/(2q\phi_{jk}^2)\,,$$

$$\lim_{q\to 0}\Gamma\equiv\delta(W_{jk})\,,$$

$$\Psi=\exp(-a_{jk}^*)(a_{jk}^*)^q/q!\,,$$

$$\Psi' = \frac{[2a^*_{jk}(1-\psi)]^{-1/2}\exp\{-(q-a^*_{jk})^2/[2a^*_{jk}(1-\psi)]\}}{\int_{-[a^*_{jk}/(2(1-\psi)]^{1/2}}^{\infty} dz\,\exp(-z^2)},$$

where S_{jk} is the probability of neuron j developing an electric potential from all synapses with neuron k, and S_j is the probability of j developing W_j from all N^* neurons. Ψ' is an alternative possibility for Ψ; ψ is defined by $a^*_{jk}=\psi e$, e the number of repetitions of an "experiment," and is likely correlated with the number of synaptic knobs.[17] This result is found to be essentially independent of the distribution taken for Ψ; i.e., Eq. (2.1) results from Ψ' as well as from Ψ [with $v^2_{jk'}\to(1-\psi)v^2_{jk'}$]. This averaging process assumes averaging over much neuronal circuitry and other microscopic details, e.g., some spatial nonadditivity and some temporal summation of postsynaptic potentials.

The large bulk of $N^*\sim 10^4$ intrinsic efferents to a neuron (extrinsic efferents are added in the next Sec. II B) originate within the extent of a "macrocolumn" $\sim 7\times 10^5\ \mu\text{m}^2$ corresponding to $\sim 10^5$ neurons.[6,16] However, clustering of interactions, synchronization and reverberation of small numbers of firing states, the greater importance of larger and more strategically placed synaptic interactions, and multiple synaptic contacts between fibers, all act to effectively reduce N^* by perhaps a factor of 2.

B. Mesocolumnar description

The neocortex has $\sim 5\times 10^{10}$ neurons distributed rather uniformly over $\sim 5\times 10^8$ minicolumns. (The visual cortex has double this density.) These columnar structures define unit modules by virtue of their afferent inputs and the nature of their processing of that input.[6] Within these minicolumns, a "vertical" structure is defined perpendicular to six highly convoluted laminae of total thickness $\sim 2.5\times 10^3\ \mu$m.[20] However, there is also a horizontal stratification to columnar interactions, and although the columnar concept has anatomical and physiological support, the minicolumnar boundaries are not so clearly defined. For instance, although minicolumns may be considered aptly as afferent modules, there is relatively much greater efferent connectivity between minicolumns within the range of a macrocolumn, rather than between two neighboring minicolumns or within a minicolumn.[21] Therefore intrinsic minicolumnar interactions within a macrocolumn of $\sim 10^3$ minicolumns might be represented well by including efferent laminar circuitry of nearest-neighbor (NN) minicolumnar interactions, next-nearest-neighbors (N^2N), . . . , and $N^{16}N$. However, given the clear anatomical and physiological support for the afferent minicolumnar module, and seeking a correct but more spatially homogeneous substrate for first study, a mesocolumn is defined here as an average afferent minicolumn (e.g., averaged over several minicolumns) of N neurons, and as an efferent average over a macrocolumn of N^* neurons efferent upon this average minicolumn.

Therefore a rough measure of divergence and convergence of columnar interactions is N^*/N, whereby a minicolumn interacts afferently via N neurons, and efferently via $\sim N^*$ axonal collaterals to a subset of its efferents as well as to other minicolumns. (If the empirically observed existence of minicolumns is arbitrarily ignored, then, as calculated in the previous Sec. II A, divergence and convergence of neuronal interactions can only be measured by that of individual neurons, which may be as high as $\sim N^*$.) The empirics of N^* and N justify the extrapolation of the global conjecture, that to facilitate communication between all neurons the number of neurons per macrocolumn in a given mammalian neocortex is approximately the square root of the total number of neocortical neurons,[22] to the more local conjecture, that to facilitate communication between all neurons within the unit of a macrocolumn $N\propto N^{*1/2}$. By including NN mesocolumnar interactions and inter-regional constraints from long-ranged fibers, a blend of these global and local optimum connectivities is formulated.

However, the functional relationships between efferent and afferent interactions are highly nonlinear, as explicitly calculated subsequently here and in Sec. II C. The following describes this averaging process calculated previously,[1] which permits a minimal homogeneous spatial scale of the extent of minicolumns to be developed for macroscopic study over regions of neocortex. In this way, stratification of interactions as well as other long-ranged input to groups of minicolumns can be included in a definition of a physiological unit consisting of one to perhaps several minicolumns, defined by its spatial-temporal excitatory (E) and inhibitory (I) afferent and efferent firing states.[1] This study formalizes these circumstances by defining a mesocolumn with extent $\rho\sim 10^2\ \mu$m, corresponding to $N\sim 100$–200 neurons, as an intermediate integral physiological unit. Dynamic nearest-neighbor interactions between mesocolumns are analytically defined by their overlapping neuronal interactions, in accordance with the observed horizontal columnar stratifications. Calculations verify that in macroscopic ac-

tivity, where mesocolumnar patterns of firing vary relatively smoothly over neighboring mesocolumns, it is consistent to approximate mesocolumnar interactions by including only second-order gradient correction terms.[1]

As derived,[1] the probability of effecting a change in firing within $\tau \geq \tau_n \sim 5$ msec in mesocolumn $M^G(r;t+\tau)$, $G=E$ or I, located at space-time point $(r;t)=(x,y;t)$ containing $N \equiv N^+ = N^E + N^I$ neurons from NN interactions with $M^{\bar{G}}(r';t)$ (scaled down from $M^{*\bar{G}}$ as discussed subsequently), $\bar{G}=E$ and I contributions, within $r'=r \leq \rho$, is

$$
\begin{aligned}
P &= \prod_G P^G[M^G(r;t+\tau) \mid M^{\bar{G}}(r';t)] \\
&= \sum_{\sigma_j} \delta\left[\sum_{jE} \sigma_j - M^E(r;t+\tau)\right] \delta\left[\sum_{jI} \sigma_j - M^I(r;t+\tau)\right] \prod_j^N p_{\sigma_j} \\
&\simeq \prod_G (2\pi)^{-1} \int_{-\infty}^{\infty} dQ^G \exp[iQ^G M^G(r;t+\tau)] \\
&\qquad \times \prod_{j \in \{G,\epsilon\}}^{N^G} [1 + |\epsilon| D_{\hat{\epsilon}}^1 + \tfrac{1}{2} |\epsilon|^2 D_{\hat{\epsilon}}^2] \cosh[F^G(r;t) + iQ^G] \operatorname{sech} F^G(r;t) \\
&\simeq \prod_G (2\pi\tau g^{GG})^{1/2} \exp(-N\tau \underline{L}^G) ,
\end{aligned}
$$

$$
\begin{aligned}
&\underline{L}^G = (\dot{M}^G - g^G)^2/(2Ng^{GG}) + M^G J_G/(2N\tau) - \underline{V}'^G , \\
&\underline{V}'^G \to \sum_{G'} \underline{V}''^G_{G'} (\rho \nabla M^{G'})^2 , \\
&\underline{V}'^G = -(2Ng^{GG})^{-1} g^G (g^G + 2M^G/\tau) dF^G , \\
&dF^G = -\tanh F^G (dF_1^G - 2 \tanh F^G dF_2^G) , \\
&dF_1^G = N^G (\rho^2/24) \alpha^G (1+\alpha^G M^+)^{-1/2} \{ -\tfrac{1}{2} F^G (1+\alpha^G M^+)^{-1/2} (\nabla^2 M^+) - \tfrac{1}{2} \beta^G (\nabla^2 M^-) \\
&\qquad + \alpha^G (1+\alpha^G M^+)^{-1} (\nabla M^+) \cdot [\beta^G (\nabla M^-) + \tfrac{3}{4} F^G (1+\alpha^G M^+)^{-1/2} (\nabla M^+)] \} , \\
&dF_2^G = N^G (\rho^2/24) (\alpha^G)^2 (1+\alpha^G M^+)^{-1} [\beta^G (\nabla M^-) + \tfrac{1}{2} F^G (1+\alpha^G M^+)^{-1/2} (\nabla M^+)]^2 ,
\end{aligned}
\tag{2.2}
$$

where τ and ρ measure the temporal and spatial scales of a mesocolumn, $M^- = M^E - M^I$, and $M^+ = M^E + M^I$. Mesocolumnar firing rates are measured by $(M^G + N^G)/(2\tau)$. $D_{\hat{\epsilon}}^{1,2}$ are directional derivatives along $\hat{\epsilon} = \epsilon/|\epsilon| = (r'-r)/|r'-r|$. The $\nabla^2 M^G$ terms are calculated by integration by parts on all factors to their left in $\underline{V}'^G$ to yield an expression proportional to $(\nabla M^G)^2$. These parameters are further defined by

$$
\begin{aligned}
&\dot{M}^G(t) = \tau^{-1}[M^G(t+\tau) - M^G(t)] , \\
&\nabla M^G(x,y) = \rho^{-1}[M^G(x+\rho,y) - M^G(x,y)]\hat{x} \\
&\qquad + \rho^{-1}[M^G(x,y+\rho) - M^G(x,y)]\hat{y} , \\
&g^G = -\tau^{-1}(M^G + N^G \tanh F^G) , \\
&g^{GG} = \tau^{-1} N^G \operatorname{sech}^2 F^G , \\
&F^G = \beta^G (\gamma^G - \alpha^G M^-)/(1+\alpha^G M^+)^{1/2} .
\end{aligned}
\tag{2.3}
$$

J_G are constraints on M^G from long-ranged fibers, and $\{\alpha^G, \beta^G, \gamma^G\}$ are six mesoscopic parameters derived from the electrical and chemical synaptic parameters averaged over a mesocolumn:

$$
\begin{aligned}
&\alpha^G = N^{*G} A^{*G}/(2N^* N^G a^{*G}) \ll 1 , \\
&a^{*G} = \tfrac{1}{2} A^{*G} + B^{*G} , \\
&\beta^G = \{N^* a^{*G} [1 + (\phi^G/v^G)^2 \pi]^{-1}\}^{1/2} < N^{*1/2} , \\
&\gamma^G = V^G/(a^{*G} v^G N^*) - N^{*-}/N^* ,
\end{aligned}
\tag{2.4}
$$

where $N^{*-} = N^{*E} - N^{*I}$, $N^* \equiv N^{*+} = N^{*E} + N^{*I}$, A^{*G} are the efficacies weighting transmission of polarization, B^{*G} are spontaneous backgrounds, v^G are postsynaptic polarizations, ϕ^G are the variances of polarizations delivered to the trigger site, and V^G are the threshold electric potentials to be exceeded to trigger presynaptic activity. The forward difference definition of $\dot{M}^G(t)$ permits $\underline{L}^G$ to possess a relatively simple functional dependence on this order parameter. I.e., P which measures the probability of transition to $M^G(t+\tau)$ from $M^G(t)$ is much more nonlinear in $M^G(t)$ than in $M^G(t+\tau)$. This is consistent with $M^G(t+\tau)$ being a firing state after interacting with efferents $M^G(t)$. Also note that, only for notational

convenience leading to facilitation of subsequent analysis, α^G are scaled parameters, thereby also causing efferent $M^G(t)$ to represent scaled firings. I.e., in the continuum limit of M^G for large N^G, $M^G(t) \equiv M^{*G}(t) N^G / N^{*G}$, $|M^G| \leq N^G$ still represent N^{*G} efferent interactions, just scaled by N^G/N^{*G}, and $\alpha^G \equiv \alpha^{*G} N^{*G}/N^G$ are still defined by averages over N^{*G} efferent and N^G afferent interactions. This scaling accomplishes the efferent definition of a mesocolumn described previously.

This development includes spatial-temporal mesocolumnar constraints, $J_G = J_G(r;t)$, from long-ranged inter-regional and extrinsic sources. These J_G constraints can also mimic other proposed chemical and electrical microscopic mechanisms that alter macroscopic firing states.[9,23,24] Empirically, $N^E{:}N^I \sim 10{:}1$, but this includes extrinsic efferents which are essentially all excitatory, comprise 5—20% of all excitatory terminals, and typically terminate on inhibitory fibers.[6] Their net effects are included in $J_G M^G$. For the remaining short-ranged interactions, considering the relative importance of inhibitory synapses (size, proximity to soma, etc.), perhaps a better ratio is $N^E{:}N^I \sim 5{:}1$.

It is known that neighboring minicolumnar interactions are predominantly inhibitory. This might be accounted for by the mesocolumnar NN's defined here as arising from overlapping efferent domains of macrocolumnar extent, with domain centers offset within the extent of a minicolumn, interacting with neighboring afferent minicolumns. As discussed previously, this definition is consistent with observations that the bulk of interminicolumnar efferents come from within the range of a macrocolumn. Therefore, it is particularly interesting that most sets of neuronal parameters to be discussed subsequently do give rise to gradient mesocolumnar NN interactions that are effectively inhibitory, i.e., they yield a net $(-)(\nabla M^E)^2$ or $(+)(\nabla M^I)^2$ contribution to $\underline{L}^E + \underline{L}^I$. Inhibitory NN interactions permit significant sharpening and identification of processed patterns across mesocolumns. Overlapping efferent domains also may be a contributing mechanism to the development of minicolumnar structure, in addition to other proposed mechanisms, e.g., two-dimensional weakly graded chemoaffinities and quasipreservation of distant mappings of neighboring efferents to neighboring afferents.

C. Macroscopic regions

This work has calculated the conditional probability that a given mesocolumn will fire, given its direct interactions with other mesocolumns just previously firing. A string of these conditional probabilities connects mesocolumnar firings at one time to the firing at any time afterwards. Many paths or strings may link given initial and final states. A Lagrangian $\tilde{L}$, the argument of the exponential expression representing the time evolution of macroscopic regions, each containing $\sim N^4$ neurons, is derived from strings of mesocolumnar conditional probabilities.[1] A major benefit derived from this formalism is a variational principle that permits extrema equations to be developed.

It is interesting that for neocortex, N, the number of neurons per mesocolumn, is large enough to permit the development of a Lagrangian macroscopic statistics; yet N is small enough for macroscopic mesocolumnar interactions to be developed as NN interactions. As determined by Eq. (2.2), N^{-1} measures the scale of fluctuations.

This Lagrangian can be expanded into a simple fourth order polynomial of powers of the mesocolumnar firings, yielding a generalized Ginzburg-Landau (GL) expression.[3] At the present stage of development of statistical mechanics, for many purposes this simple form is a practical necessity to continue future studies. This expansion is valid for the neocortical system. This also makes it possible to draw analogies to the "orienting field" and "temperature" of equilibrium collective systems. (There are also several formal developments relevant to collective equilibrium systems, based on specific GL expressions, which are not relevant to neocortex.[1]) It should be noted that some investigators have been unwilling to accept the GL analogy between ideal equilibrium and large nonequilibrium systems to describe phase transitions and long-ranged order. However, recent research demonstrates that this analogy is indeed often appropriate.[2,25–27]

Using the prior form of the short-time conditional probability, the long-time probability for global regional activity persisting for tenths of a second to seconds is derived as[1]

$$
\begin{aligned}
&\tilde{P}[\tilde{M}(t)]d\tilde{M}(t) = \int \cdots \int \underline{D}\tilde{M} \exp(-N\tilde{S}) , \\
&\tilde{S} = \int_{t_0}^{t} dt' \tilde{L} , \\
&\tilde{L} = \Lambda \Omega^{-1} \int d^2 r \underline{L} , \\
&\underline{L} = \underline{L}^E + \underline{L}^I , \\
&\underline{D}\tilde{M} = \prod_{s=1}^{u+1} \prod_{\nu=1}^{\Lambda} \prod_{G}^{E,I} (2\pi\theta)^{-1/2} (g_s^\nu)^{1/4} dM_s^{G\nu} \\
&\qquad \times \delta[M_t = M(t)] \delta[M_0 = M(t_0)] , \\
&\tilde{M} = \{M^{G\nu}\} ,
\end{aligned}
\tag{2.5}
$$

where ν labels the two-dimensional laminar $\vec{r}$-space of $\Lambda \sim 5\times 10^5$ mesocolumns spanning a typical region of neocortex, Ω (total cortical area $\sim 4\times 10^{11}\ \mu\text{m}^2$); and s labels the $u+1$ time intervals, each of duration $\theta \leq \tau$, spanning $(t-t_0)$. At a given value of $(r;t)$, it also is convenient to define $M=\{M^G\}$. The path integral in Eq. (2.5) defines M as a continuous, not necessarily differentiable, mesoscopic variable to study macroscopic regions. The "information" contained in this description is well defined as

$$\hat{Y}[\tilde{P}]=\int\cdots\int \underline{D}\tilde{M}'\tilde{P}\ln(\tilde{P}/\bar{P})\ , \qquad (2.6)$$
$$\underline{D}\tilde{M}'=\underline{D}\tilde{M}/d\tilde{M}_{u+1}\ ,$$

where $\bar{P}$ is a reference stationary state. Although many microscopic synaptic degrees of freedom have been averaged over, many degrees of freedom are still present, as measured by $dM_s^{G\nu}$. For example, neglecting specific coding of presynaptic and postsynaptic membranes, detailed neuronal circuitry, and the dynamics of temporal evolution, in a hypothetical region of 10^9 neurons with 10^{13} synapses: considering each synapse as only conducting or not conducting, there are $\simeq\exp(7\times 10^{12})$ possible synaptic combinations; considering only each neuron as firing or not firing, there are $\simeq\exp(7\times 10^8)$ neuronal combinations; considering only each mesocolumn as having integral firings between -100 and 100, there are $\simeq\exp(5\times 10^7)$ mesocolumnar combinations.

The prepoint discretization of $\underline{L}(M)$, $\theta\dot{M}(t')\to M_{s+1}-M_s$ and $M(t')\to M_s$, is derived from the biophysics of neocortex, Eqs. (2.2)–(2.4); this is not equivalent to the Stratonovich midpoint discretization of a proper Feynman Lagrangian $\underline{L}_F$, $\theta\dot{M}(t')\to M_{s+1}-M_s$ and $M(t')\to\frac{1}{2}(M_{s+1}+M_s)$.[28,29] The discretization and the Lagrangian (and g) must be consistently defined to give an invariant $\tilde{P}(\tilde{M})d\tilde{M}$. The Feynman Lagrangian is defined in terms of a stationary principle, and the transformation to the Stratonovich discretization permits the use of the standard calculus. The Einstein convention of summing over factors with repeated indices is henceforth assumed:

$$\tilde{S}_F=\min\Lambda\Omega^{-1}\int dt'\int d^2r\,\underline{L}_F\ ,$$
$$\underline{L}_F=\tfrac{1}{2}N^{-1}(\dot{M}^G-h^G)g_{GG'}(M^{G'}-h^{G'})-\underline{V}\ ,$$
$$h^G=g^G-\tfrac{1}{2}g^{-1/2}(g^{1/2}g^{GG'})_{,G'}\ ,$$
$$\underline{V}=\underline{V}'-(\tfrac{1}{2}h^G_{;G}+R/6)/N\ ,$$
$$\underline{V}'=\underline{V}'^E+\underline{V}'^I-M^GJ_G/(2N\tau)\ ,$$
$$h^G_{;G}=g^{-1/2}(g^{1/2}h^G)_{,G}\ , \qquad (2.7)$$
$$g=||g_{GG'}||=\det(g_{GG'})=g_{EE}g_{II}\ ,$$
$$g_{GG'}=(g^{GG'})^{-1}\ ,$$
$$R=g^{-1}(g_{EE,II}+g_{II,EE})-\tfrac{1}{2}g^{-2}\times\{g_{II}[g_{EE,E}g_{II,E}+(g_{EE,I})^2]+g_{EE}[g_{II,I}g_{EE,I}+(g_{II,E})^2]\}\ ,$$
$$[\cdots]_{,G}\equiv(\partial/\partial M^G)[\cdots]\ .$$

The Riemannian curvature R arises from the nonlinear inverse variance $g_{GG'}$, which is a *bona fide* metric of this parameter space[30]; $\tilde{P}(\tilde{M})d\tilde{M}$ is covariant under general $M^{G\nu}$ transformations. It has been noted that neocortex is the first physical system to be investigated with these methods that is measurably sensitive to R.[1,31]

To first order in $(\nabla M^G)^2$, the differential evolution of $\tilde{P}$ associated with Eqs. (2.5) and (2.7) is[1,29–32]

$$\frac{\partial\tilde{P}}{\partial t}=\Omega^{-1}\int d^2r[\tfrac{1}{2}\hat{\delta}_G\hat{\delta}_{G'}(g'^{GG'}\tilde{P})-\hat{\delta}_G(g'^G\tilde{P})]$$
$$\simeq\Omega^{-1}\int d^2r[\tfrac{1}{2}(g^{GG'}\tilde{P})_{,GG'}-(g^G\tilde{P})_{,G}+N\underline{V}'\tilde{P}]$$
$$=\Omega^{-1}\int d^2r(-\tfrac{1}{2}\hat{p}_G\hat{p}_{G'}g^{GG'}-i\hat{p}_Gg^G+N\underline{V}')\tilde{P}$$
$$\equiv-i\Omega^{-1}\int d^2r\,\hat{H}(\hat{p}_G,M)\tilde{P}\ ,$$
$$\hat{p}_G=-i\partial/\partial M^G\ ,$$
$$\tau g'^G\equiv\tau g^G-dF^{|G|}N^{|G|}\tanh F^{|G|}\ , \qquad (2.8)$$
$$\tau g'^{GG'}\equiv\tau g^{GG'}+\delta^{G'}_G\,dF^GN^G\operatorname{sech}^2F^G\ ,$$
$$\hat{\delta}_G[\cdots]=[\cdots]_{,G}-\nabla_z[\cdots]_{,\nabla_zG}+\nabla_z^2[\cdots]_{,\nabla_z^2G}$$
$$\equiv[\cdots]_{,G}-[\cdots]_{,G_{:z}:z}+[\cdots]_{,G_{:zz}:zz}\ ,$$
$$[\cdots]_{,G_{:z}:z}=[\cdots]_{,G_{:z}G'}M^{G'}{}_{:z}+[\cdots]_{,G_{:z}G'_{:z}}M^{G'}{}_{:zz}\ ,$$
$$[\cdots]_{:z}=\partial[\cdots]/\partial z\ ,$$
$$z=\{x,y\}\ ,$$

where vertical bars on an index, e.g., $|G|$, indicate no sum is taken over that repeated index. The Fokker-Planck functional differential equation, i.e., possessing no potential term, corresponds to the derivation in Ref. 1 of NN interactions in $\underline{L}$. However, the simpler partial differential equation arises from expansion of the ∇M^G perturbations, yielding a Schrödinger-type equation with a $\underline{V}'$ potential of NN interactions. This also defines the Hamiltonian operator $\hat{H}$. (Note that the previous discussion

modifies corresponding discussions of $\tilde{L}$ and $\hat{H}$ in Ref. 1.)

If all the $\underline{V}$ and $g^{GG'}$ in this differential equation are arbitrarily ignored, the corresponding Langevin rate equations, written in terms of "average neurons," are just those taken as the starting point for the phenomenological pioneering modeling of cortex in previous studies,[33,34] upon which most other studies are based. In some studies, simple additive noise is arbitrarily included, and then typically several thousand computer "trials" are examined to find most probable trajectories. This *ad hoc* procedure is unjustified in systems where mesoscopic fluctuations arise from intrinsic, i.e., in contrast to extrinsic sources,[35] such as occurs in neocortex. Here, the mesoscopic fluctuations are derived from the microscopic system.[1] Furthermore, a variational principle is derived to directly calculate extrema trajectories.

Numerical calculations demonstrate that, for reasonable neuronal parameters, $\tau\dot{M}^G$ and $\rho\nabla M^G$ contributions to $\underline{L}_F$ are significant but small. Therefore, it is meaningful to solve for extrema, $\langle\langle \bar{M}^G \rangle\rangle$, of $\bar{\underline{L}}_F(\bar{M})$ in terms of "uniform" $\bar{M}^G$ ($\tau\dot{\bar{M}}^G = 0 = \rho\nabla\bar{M}^G$). Minima represent most-probable firing states for $\bar{\underline{L}}_F$, and are determined by finding roots of the Euler-Lagrange variational equations, $\bar{\underline{L}}_{F,G} = 0$, such that the Hessian determinant $||\bar{\underline{L}}_{F,GG'}|| > 0$ and one of its diagonal entries $\bar{\underline{L}}_{F,|G||G|} > 0$. These uniform minima of $\bar{\underline{L}}_F$ may not be minima of $\underline{L}_F$ for all time.

In the following examples, for convenience only, N^{*G} have been scaled down to N^G, and the efficacies A^{*G} and B^{*G} have been scaled up by N^{*G}/N^G to A^G and B^G (and $a^{*G} \to a^G$). I.e., α^G, β^G, and γ^G are not affected by this scaling. This scaling is performed after the scaling in Eq. (2.4), and defines an equivalent mesoscopic system independent of N^* with the same efferent sensitivity. Table I details some representative calculations. The following notation is used to represent calculations at minima: At $\langle\langle \bar{M} \rangle\rangle$, calculate $(\bar{M}^E, \bar{M}^I; \bar{\underline{L}}_F)$, and the coefficients of $[(\nabla M^E)^2 || (\nabla M^I)^2]$ and $[(\dot{M}^E)^2 : (\dot{M}^I)^2 :: \dot{M}^E : \dot{M}^I]$ that contribute to $\underline{L}_F$. Also included are $\underline{V} - \underline{V}'$ terms at minima, illustrating that these Riemannian contributions are a measurable contribution to $\underline{L}_F$.

(Numerical calculations verify that at minima of $\underline{L}_F$, $h^G \simeq g^G$ ($h^G = g^G$ for $\gamma^G = 0$), and that $\underline{V} - \underline{V}'$ is a smooth contribution to $\underline{L}_F$. Therefore, given the realistic constraint of limited computer resources, in Ref. 1 it was decided to search for minima by minimizing $\bar{\underline{L}}$, instead of $\bar{\underline{L}}_F$ which requires processing of two orders of magnitude additional algebraic expressions. Here some of these calculations using $\underline{L}_F$ have been performed, verifying that the calculations in Ref. 1 give good estimates of those performed using $\underline{L}_F$. Also note the corrections to the $[(\nabla M^E)^2 || (\nabla M^I)^2]$ coefficients of the corresponding entries in Table I in Ref. 1. Inadvertently, coefficients of $(\nabla M^E \cdot \nabla M^I)$ were added to those of $(\nabla M^G)^2$. Coefficients of $(\nabla M^E \cdot \nabla M^I)$ are not given here since they average to zero in $\tilde{L}$, but they most likely will not average to zero when interlaminar and efferent interminicolumnar circuitries are included, as discussed in Secs. II B and III E.)

Examples A and a. Consider the following rather arbitrary example of a region of mesocolumns, each with 150 neurons, selected to model minicolumns and to symmetrize the mesoscopic parameters, with $\gamma^G = 0$. Take $N^E = 125$, $N^I = 25$, $V^G = 10$ mV, $A^G = 1.5$, $B^G = 0.25$, $v^G = \phi^G = 0.1$ mV. Contributing to $\underline{V} - \underline{V}'$ at $\langle\langle \bar{M}^G \rangle\rangle$ are the curvature $R = 0.175$ and $h^G_{;G} = 0.418$. This corresponds to example a in Ref. 1. Since $\gamma^G = 0$, $g^G = h^G$. At a scale at which gradient interactions are still small contributions, a fine structure yielding other local minima of $\underline{L}$ also becomes apparent. At the nearest integral values of $\bar{M}^G$, data at these local minima are included in Table I together with data calculated at global minima. The local minima at (6,3), (−5,−3), (8,4), and (−7,−4) have been calculated to trap firings only for integral $\langle\langle \bar{M}^G \rangle\rangle$.

Examples B and b1. The mesoscopic parameters are changed from example A, by changing the synaptic efficacies from $A^G = 1.5$ to $A^E = 1.25$ and $A^I = 1.75$. Contributing to $\underline{V} - \underline{V}'$ at $\langle\langle \bar{M}^G \rangle\rangle$ are $R = 1.06 \times 10^{-2}$ and $h^G_{;G} = -1.26$; $h^E = -5.78$ and $g^E = -5.60$; $h^I = 0.277$ and $g^I = 0.289$. This corresponds to example b1 in Ref. 1. (See Table I.)

Example b2. Example b1 is changed to $A^E = 1.75$, $A^I = 1.25$. (See Table I.)

Example c. Example b1 is changed to $N^E = 150$, $N^I = 30$. This retains the same ratio of N^E/N^I, but increases N. (See Table I.)

Example d. Example b1 is changed to $N^E = 150$, $N^I = 50$. This decreases the ratio N^E/N^I and increases N. (See Table I.)

The variational principle expressed by Eq. (2.7) straightforwardly leads to a set of 12 coupled first-order differential equations, with coefficients nonlinear in M^G, in the 12 variables $\{M^G, \dot{M}^G, \ddot{M}^G, \nabla M^G, \nabla^2 M^G\}$ in $(r;t)$ space. However, as discussed before example A, it is a good approximation to consider the nonlinear most probable firing states of $\bar{\underline{L}}$. In the neighborhood of $\langle\langle \bar{M}^G \rangle\rangle$, $\underline{L}_F$ can be expanded as a GL polynomial. To investigate first-order linear oscillatory states, only powers up to 2 in each variable are kept, and from this the variational principle leads to a relatively simple set of coupled linear differential equations

TABLE I. At minima $\langle\langle \bar{M} \rangle\rangle$, for the mesoscopic parameters given in examples A and B, calculated are $(\bar{M}^E, \bar{M}^I; \underline{\bar{L}}_F)$, the coefficients of $[(\nabla M^E)^2 || (\nabla M^I)^2]$ and $[(\dot{M}^E)^2 : (\dot{M}^I)^2 :: \dot{M}^E : \dot{M}^I]$, and the values of the Riemannian contributions $\underline{V} - \underline{V}'$ to $\underline{L}_F$. Examples a, b1, b2, c, and d are calculated using $\underline{\bar{L}}$.

$(\bar{M}^E, \bar{M}^I; \underline{\bar{L}})$	$[(\nabla M^E)^2 \|\| (\nabla M^I)^2]$	$[(\dot{M}^E)^2 : (\dot{M}^I)^2 :: \dot{M}^E : \dot{M}^I]$	$(\underline{V} - \underline{V}')$
Example A			
$(1.90, 0.939; 1.63\times10^{-3})$	$[7.37\times10^{-7} \|\| 9.71\times10^{-7}]$	$[2.67\times10^{-5} : 1.33\times10^{-4} :: -5.36\times10^{-5} : 9.57\times10^{-5}]$	-1.59×10^{-3}
Example a			
$(0,0;0)$	$[0 \|\| 0]$	$[2.67\times10^{-5} : 1.33\times10^{-4} :: 0 : 0]$	-1.68×10^{-3}
$(6,3; 4.29\times10^{-4})$	$[6.59\times10^{-6} \|\| 9.06\times10^{-6}]$	$[2.68\times10^{-5} : 1.34\times10^{-4} :: -1.58\times10^{-4} : 3.25\times10^{-4}]$	-1.41×10^{-3}
$(-5,-3; 4.52\times10^{-4})$	$[2.95\times10^{-6} \|\| 4.22\times10^{-6}]$	$[2.67\times10^{-5} : 1.34\times10^{-4} :: 6.57\times10^{-5} : -4.69\times10^{-4}]$	-1.92×10^{-3}
$(8,4; 7.54\times10^{-4})$	$[1.12\times10^{-5} \|\| 1.57\times10^{-5}]$	$[2.69\times10^{-5} : 1.35\times10^{-4} :: -2.06\times10^{-4} : 4.40\times10^{-4}]$	-1.32×10^{-3}
$(-7,-4; 7.57\times10^{-4})$	$[7.63\times10^{-6} \|\| 1.01\times10^{-5}]$	$[2.68\times10^{-5} : 1.34\times10^{-4} :: 1.29\times10^{-4} : -5.68\times10^{-4}]$	-2.03×10^{-3}
$(117.85, 23.57; 1.83\times10^{-14})$	$[-1.44\times10^{-3} \|\| 1.68\times10^{-3}]$	$[2.40\times10^{-4} : 1.20\times10^{-3} :: 3.66\times10^{-9} : 4.58\times10^{-9}]$	6.12×10^{-3}
$(-124.99, -25.00; 1.09\times10^{-10})$	$[-11.09 \|\| -0.741]$	$[1.17\times10^{-1} : 5.83\times10^{-1} :: -7.12\times10^{-6} : 0.00]$	6.66×10^{-3}
Example B			
$(94.92, 23.42; -2.25\times10^{-3})$	$[-1.15\times10^{-4} \|\| 1.14\times10^{-3}]$	$[5.45\times10^{-5} : 1.32\times10^{-3} :: 6.30\times10^{-4} : -7.33\times10^{-4}]$	4.17×10^{-3}
Example b1			
$(89.02, 23.14; 1.59\times10^{-3})$	$[-5.33\times10^{-5} \|\| 9.65\times10^{-4}]$	$[4.81\times10^{-5} : 1.09\times10^{-3} :: 5.38\times10^{-4} : -6.14\times10^{-4}]$	3.69×10^{-3}
Example b2			
$(122.69, 21.87; 1.17\times10^{-13})$	$[-5.64\times10^{-3} \|\| 1.61\times10^{-3}]$	$[7.30\times10^{-4} : 5.69\times10^{-4} :: -1.11\times10^{-8} : -1.30\times10^{-8}]$	6.77×10^{-3}
Example c			
$(21.15, 21.42; 2.38\times10^{-14})$	$[3.19\times10^{-5} \|\| 1.45\times10^{-4}]$	$[1.89\times10^{-5} : 1.89\times10^{-4} :: -1.15\times10^{-9} : -2.16\times10^{-9}]$	-9.66×10^{-4}
Example d			
$(109.48, 43.15; 1.02\times10^{-2})$	$[-3.86\times10^{-5} \|\| 6.89\times10^{-4}]$	$[2.63\times10^{-5} : 2.70\times10^{-4} :: 9.79\times10^{-4} : -1.07\times10^{-3}]$	3.28×10^{-3}

with constant coefficients:

$$0 = \hat{\delta}\underline{L}_F = \underline{L}_{F,\dot{G}:t} - \hat{\delta}_G \underline{L}_F \ ,$$

$$\simeq -\underline{f}_{|G|}\ddot{\underline{M}}^{|G|} + \underline{f}^1_G \dot{\underline{M}}^{G'} - \underline{g}_{|G|}\nabla^2 \underline{M}^{|G|} + \underline{b}_{|G|}\underline{M}^{|G|} + \underline{b}\underline{M}^{G'} \ ,$$

$$[\cdots]_{,\dot{G}:t} = [\cdots]_{,\dot{G}G'}\dot{M}^{G'} + [\cdots]_{,\dot{G}\dot{G}'}\ddot{M}^{G'} \ , \qquad (2.9)$$

$$\underline{M}^G = M^G - \langle\langle \bar{M}^G \rangle\rangle \ ,$$

$$\underline{f}^1_E = -\underline{f}^1_I \equiv \underline{f} \ .$$

These equations are then Fourier transformed and examined to determine for which values of $\{\alpha^G, \beta^G, \gamma^G\} = \{A^G, B^G, V^G, v^G, \phi^G, N^G\}$ and of $\underline{\xi}$, the conjugate variable to r, can oscillatory states, $\omega(\underline{\xi})$, persist.[1] E.g., solutions are sought of the form

$$\underline{M}^G = \mathrm{Re}\underline{M}^G_{\mathrm{osc}} \exp[-i(\underline{\xi}\cdot r - \omega t)] \ , \qquad (2.10)$$

$$\underline{M}^G_{\mathrm{osc}}(r,t) = \int d^2\underline{\xi}\, d\omega\, \hat{\underline{M}}^G_{\mathrm{osc}}(\underline{\xi},\omega)\exp[i(\underline{\xi}\cdot r - \omega t)] \ .$$

For instance, using $\underline{L}$, extrinsic sources $J_E = -2.63$ and $J_I = 4.94$ drive the global minima of example b2 to $\bar{M}^E = 25$ and $\bar{M}^I = 5$, and yield dispersion relations

$$\omega\tau = \pm\{-1.86 + 29.6(\xi\rho)^2; -1.25i + 18.7i(\xi\rho)^2\} \ , \qquad (2.11)$$

$$\xi = |\underline{\xi}| \ .$$

The boundary conditions in Eq. (2.5) further specify these solutions. In those regions where real ω exist, wave propagation velocities, $\hat{v}$, are determined by $d\omega/d\xi$. Several different mesocolumnar mechanisms, defined by the influences of the $\underline{b}$, $\underline{f}$, and $\underline{g}$ coefficients in Eq. (2.9), can produce real wave propagation rates. Examples are manufactured straightforwardly.

Table I demonstrates that even modest changes in A^G or N^G cause dramatic shifts in $\langle\langle \bar{M}^G \rangle\rangle$ and in properties of $\underline{M}^G$ solutions to Eq. (2.9). This is a highly nonlinear system, even after taking mesocolumnar averaged parameters. The closest example to linearity arises in the special case of $\gamma^G \simeq 0$ and

$M^E \simeq M^I$, when the mean $\tau \dot{M}^G \simeq N^G \beta^G (\alpha^G M^G - \gamma^G) - M^G$. More generally, even if $\dot{M}$, ∇M, and $\underline{V} - \underline{V}'$ terms are neglected, a true minimum is often determined by competition between the two conditions, $0 = M^G + N^{|G|} \tanh F^{|G|}$, each weighted by its variance $g^{GG} = \tau^{-1} N^{|G|} \mathrm{sech}^2 F^{|G|}$. Furthermore, as demonstrated,[1] there are often multiple minima, which will eventually require more detailed studies of subharmonic (period-doubling) bifurcations, phase transitions and fluctuations.[3,36]

A complete GL expression for $\underline{L}$ is derived for example b1:

$$\begin{aligned}
\tau \underline{L} \simeq\ & 1.59\times10^{-3} - 5.33\times10^{-5}(\nabla \underline{M}^E)^2 + 9.65\times10^{-4}(\nabla \underline{M}^I)^2 + 4.81\times10^{-5}(\dot{\underline{M}}^E)^2 + 1.09\times10^{-3}(\dot{\underline{M}}^I)^2 \\
& - 9.05\times10^{-7}\underline{M}^E\dot{\underline{M}}^E + 2.37\times10^{-3}\underline{M}^I\dot{\underline{M}}^I - 1.45\times10^{-4}\underline{M}^E\dot{\underline{M}}^I + 1.12\times10^{-4}\dot{\underline{M}}^E\underline{M}^I \\
& + 5.38\times10^{-4}\dot{\underline{M}}^E - 6.14\times10^{-4}\dot{\underline{M}}^I + 1.15\times10^{-5}(\underline{M}^E)^2 - 1.72\times10^{-4}\underline{M}^E\underline{M}^I \\
& + 1.36\times10^{-3}(\underline{M}^I)^2 - 5.91\times10^{-8}(\underline{M}^E)^3 - 7.44\times10^{-7}(\underline{M}^E)^2\underline{M}^I \\
& + 4.29\times10^{-5}\underline{M}^E(\underline{M}^I)^2 - 5.43\times10^{-5}(\underline{M}^I)^3 + 8.67\times10^{-9}(\underline{M}^E)^4 - 3.96\times10^{-8}(\underline{M}^E)^3\underline{M}^I \\
& + 7.64\times10^{-7}(\underline{M}^E\underline{M}^I)^2 - 1.99\times10^{-6}\underline{M}^E(\underline{M}^I)^3 + 1.38\times10^{-6}(\underline{M}^I)^4 \ .
\end{aligned} \tag{2.12}$$

$M^G \simeq 0$ is the range of maximum redundancy of mesocolumnar firing; i.e., there are more combinations giving $M^G = 0$ than any other firing state.[1] Therefore, when suitably constrained by J_G, e.g., $J_E = 1.27$ and $J_I = -1.12$ drive $\langle\langle \bar{M}^G \rangle\rangle$ to 0 for example b1, this is the range most likely to induce plastic synaptic modifications, e.g., during development. The GL polynomial for this state is

$$\begin{aligned}
\tau \underline{L} \simeq\ & 0.0970 + 4.24\times10^{-4}(\nabla \underline{M}^E)^2 + 3.39\times10^{-4}(\nabla \underline{M}^I)^2 + 3.20\times10^{-5}(\dot{\underline{M}}^E)^2 + 1.54\times10^{-4}(\dot{\underline{M}}^I)^2 \\
& - 1.49\times10^{-4}\underline{M}^E\dot{\underline{M}}^E + 5.51\times10^{-4}\underline{M}^I\dot{\underline{M}}^I - 2.26\times10^{-4}\underline{M}^E\dot{\underline{M}}^I + 1.94\times10^{-4}\dot{\underline{M}}^E\underline{M}^I \\
& + 3.28\times10^{-3}\dot{\underline{M}}^E - 2.82\times10^{-3}\dot{\underline{M}}^I + 2.14\times10^{-4}(\underline{M}^E)^2 - 7.38\times10^{-4}\underline{M}^E\underline{M}^I \\
& + 7.19\times10^{-4}(\underline{M}^I)^2 - 1.01\times10^{-6}(\underline{M}^E)^3 - 1.06\times10^{-6}(\underline{M}^E)^2\underline{M}^I \\
& + 1.00\times10^{-5}\underline{M}^E(\underline{M}^I)^2 - 8.30\times10^{-6}(\underline{M}^I)^3 + 2.42\times10^{-8}(\underline{M}^E)^4 - 1.92\times10^{-7}(\underline{M}^E)^3\underline{M}^I \\
& + 6.09\times10^{-7}(\underline{M}^E\underline{M}^I)^2 - 7.89\times10^{-7}\underline{M}^E(\underline{M}^I)^3 + 3.52\times10^{-7}(\underline{M}^I)^4 \ .
\end{aligned} \tag{2.13}$$

The measure $\underline{D}\tilde{M}$ in Eq. (2.5) contains a weighting factor $g^{1/2}$ which is also expanded and included in an effective Lagrangian $\underline{L}_{\mathrm{eff}}$. For brevity, to second order,

$$\underline{L}_{\mathrm{eff}} = \underline{L} + (N\tau)^{-1} \ln(\tau g^{-1/2}) \ , \tag{2.14}$$

$$\begin{aligned}
\tau^{-1} g^{1/2} \simeq\ & 0.0211 + 2.76\times10^{-6}\underline{M}^E - 3.60\times10^{-5}\underline{M}^I + 1.06\times10^{-5}(\underline{M}^E)^2 - 2.13\times10^{-5}\underline{M}^E\underline{M}^I \\
& + 1.10\times10^{-5}(\underline{M}^I)^2 \ .
\end{aligned}$$

These polynomial expansions, besides being starting points for more detailed investigations, also serve to explicitly display simple functional forms that can be directly used or truncated after the nonlinear eikonals are calculated. This specificity is necessary if theoretical and experimental investigations are to eventually merge. More intuitive insights are gained by examining three-dimensional plots of spatially temporally averaged $\bar{\underline{L}}$ versus $\bar{M}^G$ at various resolutions.[1]

D. Corrections to previous modeling of neocortex

Many previous theoretical studies and computer simulations that have modeled neural systems have been careful to initially describe the empirical situation, but unfortunately they have also often arbitrarily and erroneously used simple linear differential rate equations for "average neurons" as the essential underlying foundation of their specific calculations, thereby opening to question the net validity of their results. It is understandable that a relatively simple set of readily solvable differential equations is required for many models and modelers. However, it is clearly better to be consistent with the actual empirical situation, e.g., by attempting to use a set of Langevin rate equations corresponding to the Schrödinger-type equation (2.8). This still would not add much labor to existing computer calculations.

This might be achieved in the following manner: For a given set of neuronal parameters, within a

neighborhood of an established set of minima, it might be possible to have the contributions to the potential from $M^G J_G$ be simulated by appropriate boundary conditions. This is sometimes possible.[19] E.g., if the effect of J_G is known beforehand to simply shift $\langle\langle \overline{M}^G \rangle\rangle$, then these "boundary conditions" are essentially accounted for by writing all expressions in terms of $\underline{M}^G = M^G - \langle\langle \overline{M}^G \rangle\rangle$, and considering all calculations to take place in a neighborhood of $\langle\langle \overline{M}^G \rangle\rangle$. If this hurdle could be overcome, then the ensuing Fokker-Planck equation can be written with $\underline{V}=0$ in Eq. (2.8). If only most probable *transition* states are sought, simple coupled first-order rate equations are given by[37]

$$\begin{aligned} \dot{M}^G &= g'^G - \tfrac{1}{2} g'^{1/2} (g'^{-1/2} g'^{GG'})_{,G'} , \\ g' &= (\det g'^{GG'})^{-1} , \end{aligned} \tag{2.15}$$

where g'^G and $g'^{GG'}$ are defined in Eq. (2.8).

However, if fluctuations are required, these can be included in the coupled Langevin rate equations corresponding to Eq. (2.8) with $M^G J_G$ simulated by boundary conditions. The Langevin equations in the Stratonovich representation are

$$\begin{aligned} &\dot{M}^G = g'^G - \tfrac{1}{2} \delta^{jk} \hat{g}_j^{G'} \hat{g}_{k,G'}^G + \hat{g}_j^G \eta_j , \\ &\hat{g}_j^G \hat{g}_k^{G'} \delta^{jk} = g'^{GG'}/\tau , \\ &\langle \eta_i(t) \rangle = 0 , \\ &\langle \eta_i(t) \eta_j(t') \rangle = \delta_{ij} \delta(t-t') , \end{aligned} \tag{2.16}$$

where η_j represents Gaussian white noise arising from the microscopic neuronal system labeled by j. Because of the derivations in Secs. II A and II B, it is reasonable to take $\hat{g}_j^G \simeq \delta_{G'}^G [g'^{GG'}/(N^G \tau)]^{1/2}$, $j=1, \ldots, N$ and $j \in G$; $\hat{g}_j^G = 0$, $j \in G' \neq G$.

Equations (2.15) and (2.16) also may be rewritten for individual mesocolumnar-averaged neurons, m^G, by setting $M^G = N m^G$. The terms dF^G, defined in Eq. (2.2), appear in accordance with their derivation,[1] and they may be retained to include intercolumnar interactions. F^G, defined in Eq. (2.3), and dF^G may be further simplified to linear terms in $\underline{M}^G = M^G - \langle\langle \overline{M}^G \rangle\rangle$, expanded about minima $\langle\langle \overline{M}^G \rangle\rangle$ after these are correctly calculated.

In the neighborhood of minima $\langle\langle \overline{M}^G \rangle\rangle$, the coefficients of $\underline{M}^G$ in rate equations may be substantially altered, e.g., by a factor ranging from 10^{-2} to 10^2. As deduced by scaling these equations to set the $\underline{M}^G$ coefficients = 1, this essentially radically changes the effective time scale of $\tau \sim 5-10$ msec assumed in previous studies by this factor. Also, the "noise" contribution is multiplicative, not simply additive as has been assumed in previous studies.

III. DYNAMICS OF SYNAPTIC MODIFICATION

A. Firing patterns and synaptic modifications

There are several new and useful features to be added to neocortical description by this formalism:

Depth and breadth of processing. The sharpness of the mean rate of firings, the depth of information processing, is measured by the "step-function" $\tanh F^G$, where the "threshold function" F^G is sensitive to a factor of $N^{*1/2}$. The strength of coupling between mesocolumns, the breadth of information processing, measured by the potential term $\underline{V}'$, is roughly proportional to a factor of $NN^{*1/2}$. It is noted that visual cortex possesses twice the density of neurons per mesocolumn as other cortical regions,[6] and therefore is better suited than other regions to process large patterns of detailed information. Calculations of formation, stability, hysteresis, and interaction of patterns of firings, upon which are based other calculations describing plastic synaptic modifications, exhibit this dependence on these depth and breadth dimensions.

Columnar development and processing. Using the variational principle, most-probable firings can be simply calculated even in the presence of highly nonlinear means and variances. Because both temporal and spatial differentials have been developed, space-time properties of these most-probable states are easily examined. For example, for some reasonable values of synaptic parameters, oscillatory states are found for small space-time fluctuations. There exist many sets of gradient couplings in $\underline{V}'$ that cause nearest-neighbor mesocolumns to fire M^E (M^I) oppositely (similarly), in accord with empirical observations that favor periodically alternating columnar organization.[38-42]

An interesting set of hypotheses of columnar development and physiology is immediately suggested: Synaptic stimulation of fibers is most likely necessary for trophic as well as communicative purposes,[43] and during early development extrinsic stimulation is necessary[44] but probably relatively nonspecific, statistically favoring the observed alternating columnar development. In mature cortex, extrinsic regional stimulation by a given extrinsic source, J_G, is sufficient to stimulate all columns in a region to facilitate nonspecific global attention[45,46] in preparation for pattern formation, as well as to facilitate specific selective attention and processing, e.g., by increasing the signal-to-noise ratio. This shift in columnar activity would be parallel to shifts in sensitivity during selective attention noted in individual neurons, which exhibit a decrease in spontaneous activity due to their extrinsic stimulation, modeled here by B_{jk}^*.

Plastic synaptic modifications can develop new sets of eigenfunctions of firing states which retain the information from these sets of external stimulation, if they can reproduce and sustain the externally induced most-probable firing patterns and their associated set of eigenfunctions. Induced chemical and developmental processes, several of which are conjectured in the literature,[23,24] may be considered to have evolved to permit the columnar system to achieve its most-probable firing states which are commensurate with the mesocolumnar firings calculated before. Further, these firing states may provide favorable statistical backgrounds to facilitate the development of specific neuronal pathways that also have been hypothesized to process information.[11,47]

Latency and spatial extent of pattern formation. With regard to pattern formation, latencies of evoked potentials[8] and fields[10] on the order of hundreds of milliseconds most likely involve delays due to slower short-ranged mesocolumnar interactions, despite faster long-ranged axonal propagation of impulses at rates of 600—900 cm/sec, larger myelinated fibers affording faster transportation of action potentials.[9] It has been noted that phase changes of evoked fields often only occur over distances greater than several centimeters, on the scale of a region, so that long wavelength low-frequency processing, sufficient to process patterns of information involves many columnar interactions requiring long temporal and spatial coherencies of short-time and short-ranged interactions. These latencies and spatial extents can be explicitly calculated, e.g., as propagation rates of information processing as calculated in Sec. II. These latencies also express the long temporal scales necessary, albeit not sufficient, to favor plastic synaptic modifications.

Calculation of pattern interactions. A large literature deals with information processing of neural networks, but the experimental and theoretical values of their conclusions are generally diminished because they do not properly include relatively fundamental synaptic interactions or properly treat nonlinear and nonequilibrium aspects of neocortex.[7,48–50] Once the information states referred to by these authors have been calculated and or tabulated, then their proposed mechanisms and conclusions can be tested. For example, an eigenfunction expansion of the probability function derived in Sec. II, into a set of spatial-temporal solutions, provides a mathematical framework to rigorously discuss pattern formation, stability, and interactions, e.g., short-term and long-term memory, nonassociative learning (habituation and sensitization) and associative learning (classical and operant conditioning), the latter especially requiring temporal correlations. This is a straightforward, albeit modest, computer project, similar to that accomplished in other physical problems possessing gradient ("momentum-dependent") potentials, e.g., in nuclear physics[51]; i.e., the "momentum" operators $\hat{p}_G$ in Eq. (2.8) operate on nonconstant factors multiplying $\tilde{P}$.

As calculated, simple localized or oscillatory patterns exist for specific mesoscopic parameters in regions of small spatial-temporal fluctuations, but nonlinearities and fluctuations now can and should be included to perform more definitive calculations. For example, overlaps of eigenfunctions from different sets of mesocolumnar parameters can measure the formation and stability of patterns of plastic changes in presynaptic and postsynaptic parameters.[52]

B. Synaptic modifications coding extrinsic stimuli

Section II describes the nonlinear nonequilibrium dynamics of patterns of mesocolumnar firings, formulated in terms of mesocolumnar-averaged static neuronal parameters. Perturbations of these parameters correspond to plastic synaptic modifications, associated with new firing minima and their associated sets of eigenfunctions, related to learning new sets of information. Especially during development of synaptic formation, at a rate determined by successive small increments of these perturbations, changes in the coefficients of gradient couplings also represent shifts in oscillatory states and in the degree of interaction between columnar firings.

To further clarify this methodology, an explicit calculation is given, demonstrating how a small increment of extrinsically imposed firing activity can be learned and stored as plastic synaptic modifications. Moderate changes in efficacies of even one neuron per mesocolumn give rise to moderate changes in macroscopic activity, and therefore it is proposed that macroscopic measurements can be sensitive to microscopic details of neocortical interactions.

Consider the change in probability of firing of neuron j, p_{σ_j}, associated with modifications of the neuronal parameters that enter Eq. (2.1). For example, changes can occur in

$$Z=\{A^*_{jk},B^*_{jk},V_j,v_{jk},\phi_{jk},N^{*E},N^{*I}\} \tag{3.1a}$$

which leads to

$$Z+\Delta Z=Z+\{\Delta A^*_{jk},\Delta B^*_{jk},\Delta V_j,\Delta v_{jk},\Delta\phi_{jk},\Delta N^{*E},\Delta N^{*I}\}\ , \tag{3.1b}$$

where changes in each parameter Z, ΔZ, can be independent or proportional to the (repeated) firing of neuron(s) postsynaptically (j) or presynaptically (k):

$$\Delta Z=\Delta Z_1+\sigma_k\Delta Z_2+\sigma_k\sigma_j\Delta Z_3+\sigma_j\Delta Z_4 \ . \quad (3.2)$$

More theory and experiments are needed to further detail the biophysics[53] and biochemistry[54] of $\Delta Z_{1,2,3,4}$.

All these ΔZ effects collect to modify

$$F_j\rightarrow F_j'=F_j+(\Delta F_{j1}+\Delta F_{j2})+\sigma_j(\Delta F_{j3}+\Delta F_{j4}) \ . \quad (3.3)$$

To order $\Delta F_{j1,2,3,4}$, to preserve the normalization of probability, $p_+ +p_- =1$, it is derived that p_{σ_j} is modified as

$$p_{\sigma_j}\rightarrow p_{\sigma_j}'=\exp(\sigma_j F_j'')/[\exp F_j''+\exp(-F_j'')] \ , \quad (3.4)$$

$$F_j''=F_j+\Delta F_{j1}+\Delta F_{j2}-(\Delta F_{j3}+\Delta F_{j4})\tanh F_j \ .$$

Thus, the change in response of a single neuron associated with its synaptic modifications is a highly nonlinear function of the synaptic parameters $\{Z,\Delta Z\}$. Nonlinearities persist even after mesocolumnar averaging, but then, because of the derived variational principle, explicit calculations can be performed to portray most-probable changes in patterns of columnar firings associated with changes in the Lagrangian:

$$\underline{L}_F\rightarrow\underline{L}_F+\Delta\underline{L}_F\simeq\underline{L}_F+\sum_Z\frac{\partial\underline{L}_F}{\partial Z^G}\Delta Z^G \ . \quad (3.5)$$

To emphasize the point that linear response models of neuronal activity should be scrutinized with respect to the biophysics and mathematics they are assuming to be linear, the following equation represents the first-order change in $\underline{L}$, Eq. (2.5), associated with modifications of only the columnar averaged efficacies A^G:

$$\begin{aligned}
\Delta\underline{L}&=\Delta F^G(2N^GN\tau)^{-1}\{[(N^G)^2+(\tau\dot{M}^G+M^G)^2]\sinh(2F^G)+2N^G(\tau\dot{M}^G+M^G)\cosh(2F^G)\}\\
&\quad-\Delta A^G(\partial\underline{V}''^G_{G'}/\partial A^G)(\rho\nabla M^{G'})^2 \ ,\\
\Delta F^G&=-(2F_d^G)^{-1}\Delta A^G[v^G(M^-+N^-)+\pi(v^{G2}+\phi^{G2})(M^++N^+)F^G/(2F_d^G)] \ , \quad (3.6)\\
F_d^G&=[\pi(v^{G2}+\phi^{G2})(A^GM^+/2+a^GN^+)]^{1/2} \ ,\\
\Delta A^G&=\Delta A_1^G+\Delta A_2^G-(\Delta A_3^G+\Delta A_4^G)\tanh F^G \ .
\end{aligned}$$

Examining ΔA^G in Eq. (3.6), it is clear that even after mesocolumnar averaging, groups of synaptic modifications dependent on postsynaptic firings can be discerned from groups of modifications independent of this activity, by the additional $\tanh F^G$ factor. However, mesocolumnar averaging washes out discrimination of $\Delta A_{1,3}^G$ from $\Delta A_{2,4}^G$ unless these possess additional distinguishing functional features. Similar calculations are proposed to further investigate phenomena as encountered in habituation.[43]

For instance, if the system described by example b1 is synaptically modified about its most probable firing state by $\Delta A_3^E=0.01$ [requiring modification by $-\tanh F^G$ as in Eq. (3.6)], e.g., numerically equivalent to a substantial change in A_{jk} of one E neuron per mesocolumn in a region, then the change in the uniform Lagrangian is

$$\begin{aligned}
\tau\Delta\underline{\bar{L}}\simeq&-4.87\times10^{-4}+3.99\times10^{-6}(\overline{M}^E-\langle\langle\overline{M}^E\rangle\rangle)\\
&-9.80\times10^{-5}(\overline{M}^I-\langle\langle\overline{M}^I\rangle\rangle) \ . \quad (3.7)
\end{aligned}$$

The shifts in the most-probable firing state $\langle\langle\overline{M}^G\rangle\rangle$ associated with this synaptic modification are observed to be algebraically equivalent, within a constant increment to $\underline{L}$, to those that could also have been caused by extrinsic stimulations measured by $J_E/(2\tau N)=3.99\times10^{-6}$ and $J_I/(2\tau N)=-9.80\times10^{-5}$. This shifts $\langle\langle\overline{M}^G\rangle\rangle$ and $\underline{\bar{L}}$ from $(89.02,23.14;1.59\times10^{-3})$ (see Table I) to $(89.20,23.19;-3.25\times10^{-4})$, and changes the derivative coefficients to $[-5.72\times10^{-5}||9.65\times10^{-4}]$ and $[4.82\times10^{-5}:1.10\times10^{-3}::5.43\times10^{-4}:-5.28\times10^{-4}]$. $\omega\tau$ is shifted from $\pm\{0.392i-1.68i(\xi\rho)^2;1.01i-0.541i(\xi\rho)^2\}$ to $\pm\{0.396i-1.79i(\xi\rho)^2;1.01i-0.550i(\xi\rho)^2\}$. These numbers indicate that the sensitivity of mesocolumnar statistics to microscopic dynamics is barely within the present range of experimental determination.

This calculation also represents an explicit demonstration of how extrinsic constraints on firing patterns can be learned and coded by plastic synaptic modifications. In general, there exist (a set of) synaptic modifications $\Delta Z(r;t')$ that reproduce the most probable firing states $\langle\langle\overline{M}(t')\rangle\rangle$ induced by $J_G(r;t')$. The examples in Table I also serve to demonstrate that relatively larger shifts in ΔZ represent highly nonlinear changes in firing patterns.

It is interesting to take both local and global views of the influences of J_G on extrema $\langle\langle\overline{M}^G\rangle\rangle$, as typically large ranges of $\langle\langle\overline{M}^G\rangle\rangle$ appear to have sim-

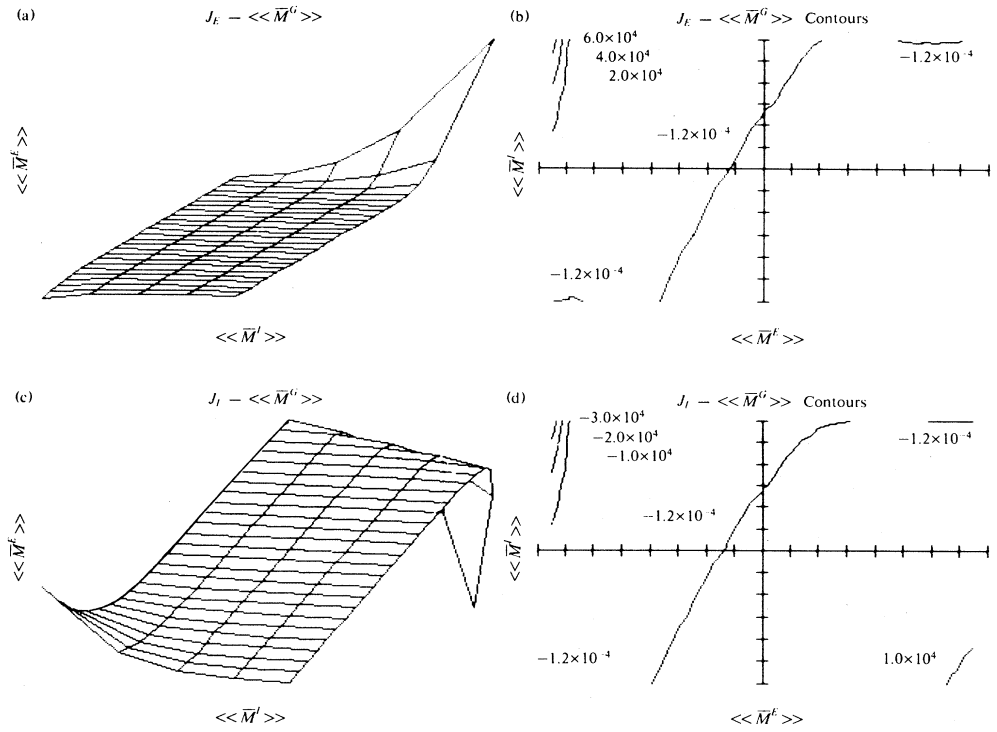

FIG. 2. In (a) and (c), a distant view is taken of J_G versus $\langle\langle \bar{M}^G \rangle\rangle$. This is determined in terms of min $= (\langle\langle \bar{M}^E \rangle\rangle_{\min}, \langle\langle \bar{M}^I \rangle\rangle_{\min}, J^G_{\min})$ and max $= (\langle\langle \bar{M}^E \rangle\rangle_{\max}, \langle\langle \bar{M}^I \rangle\rangle_{\max}, J^G_{\max})$. The plots are projected onto a plane perpendicular to the line running between a point on the line of sight, chosen here to be (min + max)/2, and the point from which the projection is made, chosen here to be max+3(max−min). For this example c, $\langle\langle \bar{M}^E \rangle\rangle_{\min} = -150$, $\langle\langle \bar{M}^E \rangle\rangle_{\max} = 150$, $\langle\langle \bar{M}^I \rangle\rangle_{\min} = -30$, and $\langle\langle \bar{M}^I \rangle\rangle_{\max} = 30$. The horizontal $\langle\langle \bar{M}^I \rangle\rangle$ axes increase to the right, and the sloping $\langle\langle \bar{M}^E \rangle\rangle$ axes increase down towards the left. Contour plots in (b) and (d) are of J_G vs $\langle\langle \bar{M}^E \rangle\rangle$, on the horizontal axis increasing to the right, and $\langle\langle \bar{M}^I \rangle\rangle$, on the vertical axis increasing upwards.

ple functional relationships to J_G. Figure 2 illustrates three-dimensional and contour plots for example c, using $\underline{L}$, of values of J_G necessary to establish extrema $\langle\langle \bar{M}^G \rangle\rangle^{J_G}$, viewed from a large enough distance to avoid much perceptual convergence. Figure 3 gives a closer look at a rather smooth fine structure relevant to neocortex by examining a small range of Fig. 2 about $\langle\langle \bar{M}^G \rangle\rangle^{J_G=0}$ for example c.

Maxima and minima of $\bar{\underline{L}}$ are conveniently ascertained by examining the Hessian (H) of $\bar{\underline{L}}$. For $H>0$ and $-2N\bar{\underline{L}}_{,EE} = J_{E,E}$ (or $J_{I,I}$) <0, $\bar{\underline{L}}$ has a local minimum; if $H>0$ and $-2N\bar{\underline{L}}_{,EE}>0$, $\bar{\underline{L}}$ has a local maximum; else if $H<0$, a local extremum does not exist. Figure 4 gives contour plots of $4N^2H$, to be consistent with the scalings in Figs. 2 and 3, and of $J_{E,E}$.

Thus, although the dependency of $\langle\langle \bar{M}^G \rangle\rangle$ on M^G is highly nonlinear, the interaction between $\langle\langle \bar{M}^G \rangle\rangle$ and J_G is only mildly nonlinear. This explicitly defines how the macroscopic interaction of most-probable firing patterns with extrinsic sources, still sensitive to microscopic circuitries, is a smoother phenomenon than the mesoscopic and microscopic responses to these sources. Note that a selected pair of $\langle\langle \bar{M}^G \rangle\rangle$ defines a pair of J_G uniquely, but this mapping is not globally one to one: It is possible that different pairs of J_G may induce the same extrema $\langle\langle \bar{M}^G \rangle\rangle$. Furthermore, it may be expected that when spatial-temporal variations are included in the full $\underline{L}_F$ Lagrangian, there will be even more nonlinearity in the interaction between $J_G(r;t')$ and $\langle\langle \tilde{M}(t') \rangle\rangle$.

C. Hysteresis of firing patterns

It is generally conceded that a short-term memory mechanism is necessary, albeit not sufficient, for long-term stability of coding to take effect.[43] Hysteresis of firing patterns encoding information is a possible mechanism. This also has been suggested as a mechanism for other neocortical phenomena.[3,55] For hysteresis to be prominent, the typical period within which synaptic parameters are altered, e.g., alterations of ΔZ in Eqs. (3.1) due to changes in ex-

trinsic J_G, should be much greater than the relaxation period of M^G, but much less than the decay period for the system to jump and or fluctuate between competing minima $\langle\langle M^G\rangle\rangle$. Figures 2–4 specifically illustrate how stationary $\langle\langle \bar{M}^G\rangle\rangle$ of $\underline{L}$ shift with J_G, and Eq. (3.7) illustrates how these shifts may be coded by ΔZ.

Time scales on which jumps between competing minima take place can be estimated by calculating the time of first passage between competing minima of $\underline{L}_F$,[25] given by $-\int_0^\infty dt\, t(\partial P/\partial t)$. Example a, with the seven minima listed in Table I, can be examined to estimate times of first passage. For this example a very good estimate of a stationary solution P_{stat} to the Fokker-Planck Eq. (2.8) for an uncoupled mesocolumn, i.e., $\underline{V}'=0$, is given by

$$P_{\text{stat}} \simeq N_{\text{stat}} \exp(-N\tau \underline{\bar{L}}) , \tag{3.8}$$

where N_{stat} is the stationary normalization. Nonconstant corrections from $g^{GG'}$ are ignored for this estimate, and also taken into consideration is that $\underline{\bar{L}}^E \sim (N^E/N^I)\underline{\bar{L}}^I$. This effectively reduces the calculation to a one-dimensional linearized Fokker-Planck equation along a trajectory connecting the minima. Then, using this stationary solution and the Fokker-Planck equation, the time for first passage, t_{vp}, is calculated as

$$\frac{t_{vp}}{\tau} \simeq \pi \left[\frac{||\underline{\bar{L}}_{,GG'}(\langle\langle \bar{M}\rangle\rangle_p)||}{||\underline{\bar{L}}_{,GG'}(\langle\langle \bar{M}\rangle\rangle_v)||} \right]^{1/2} \times \exp\{N\tau[\underline{\bar{L}}(\langle\langle \bar{M}\rangle\rangle_p) - \underline{\bar{L}}(\langle\langle \bar{M}\rangle\rangle_v)]\} , \tag{3.9}$$

where $\langle\langle \bar{M}\rangle\rangle_v$ is the minimum at the valley of $\underline{\bar{L}}$ in question, and $\langle\langle \bar{M}\rangle\rangle_p$ is the maximum at a peak separating two minima.

The exponential factor in Eq (3.9) can be quite large in some instances, and quite small in others. Figure 5 gives some contour plots of example a which illustrate this point. Values of $\tau\underline{\bar{L}}$ at maxima between the five minima clustered about the global minimum $\langle\langle \bar{M}^G\rangle\rangle=(0,0)$ are on the order of 0.01 and therefore only contribute an argument on the order of unity to this exponential factor. [This calculation could be extended to consider pairs of minima clustered about (0,0) being close enough to warrant a critical point treatment.[25]] As noted in Table I, differences in $\underline{\bar{L}}$ from valleys to peaks are still large relative to the Riemannian correction terms

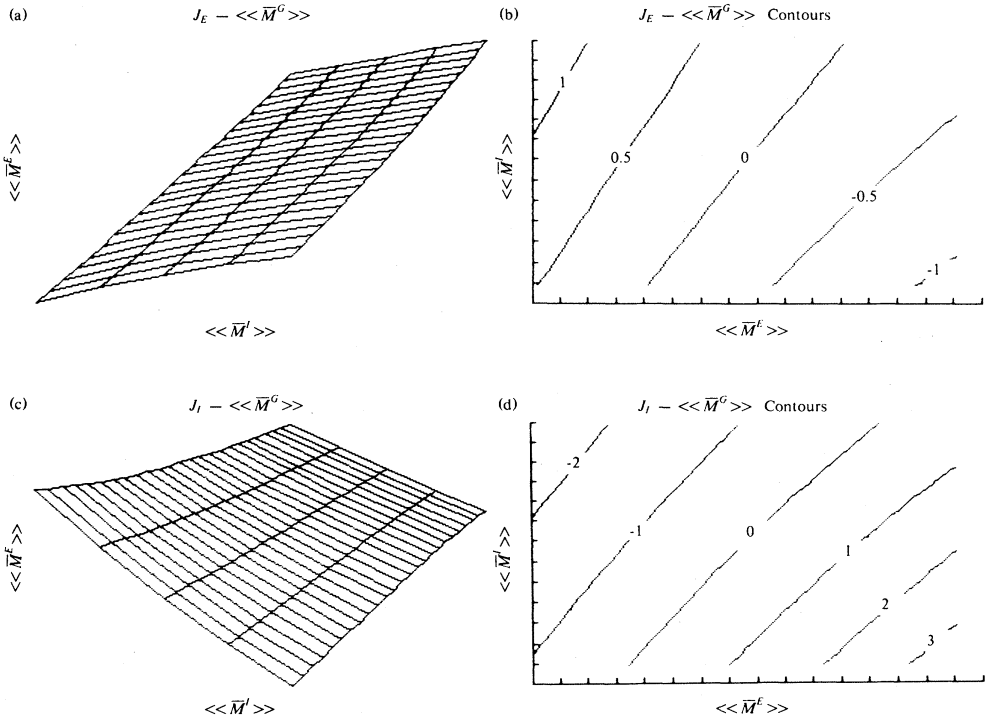

FIG. 3. A closer look at the plots in Fig. 2 reveals a fine structure relating J_G to extrema $\langle\langle \bar{M}^G\rangle\rangle^{J_G}$. Axes run similar to those in Fig. 2, but here $\langle\langle \bar{M}^E\rangle\rangle_{\min}=\langle\langle \bar{M}^E\rangle\rangle^{J_G=0}-15$, $\langle\langle \bar{M}^E\rangle\rangle_{\max}=\langle\langle \bar{M}^E\rangle\rangle^{J_G=0}+15$, $\langle\langle \bar{M}^I\rangle\rangle_{\min}=\langle\langle \bar{M}^I\rangle\rangle^{J_G=0}-3$, and $\langle\langle \bar{M}^I\rangle\rangle_{\max}=\langle\langle \bar{M}^I\rangle\rangle^{J_G=0}+3$, where for this example c, $\langle\langle \bar{M}^G\rangle\rangle^{J_G=0}=(21.15,21.42)$.

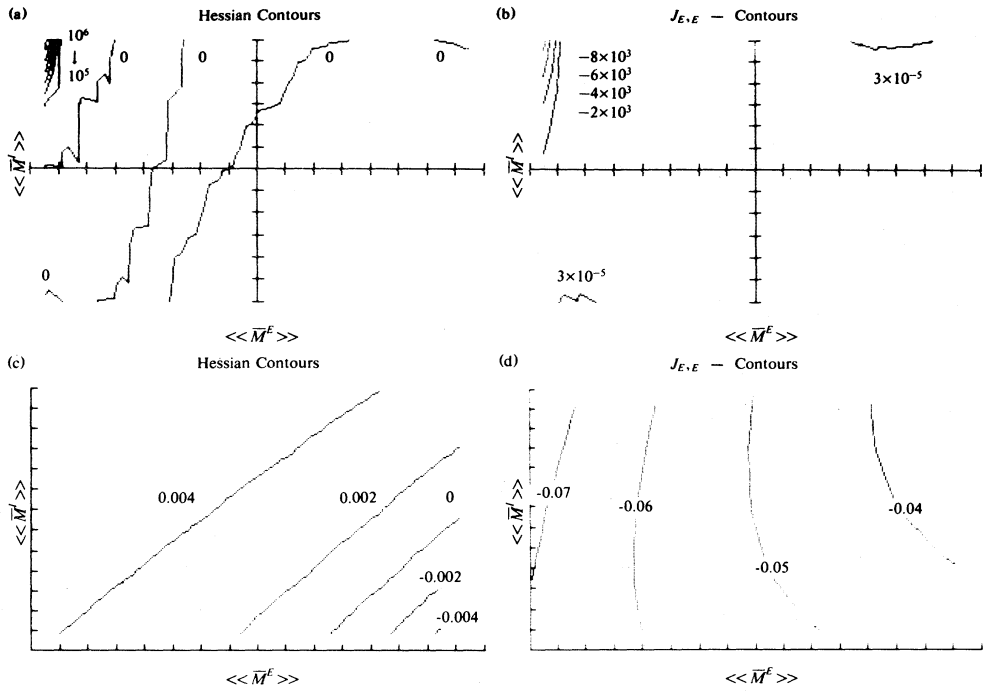

FIG. 4. Contour plots are given of $4N^2H=4N^2||\underline{\bar{L}}_{,GG'}||$, and of $-2N\underline{\bar{L}}_{,EE}=J_{E,E}$ for example c. Plots (a) and (b) correspond to the scaling of Fig. 2, and plots (c) and (d) correspond to the scaling of Fig. 3. In plot (a), the upper left contours range from 1.2×10^6 down to 2×10^5, in decrements of 2×10^2; if more contours were plotted, some of value $\sim-10^{-5}$ would appear about those at 0. In plot (b), if more contours were plotted, some of value $\sim-10^{-6}$ would appear about those at 3×10^{-5}.

and relative to differential spatial-temporal contributions, thereby permitting this analysis. However, values of $\underline{\bar{L}}$ at maxima between the far minima near maximal and minimal $\langle\langle\bar{M}^G\rangle\rangle$ firings, or between minima clustered about (0,0) and minimal $\langle\langle\bar{M}^G\rangle\rangle$ firings, are >1, thereby contributing an argument on the order of 10^2 to this exponential, yielding an enormous t_{vp}, typical of many physical systems undergoing hysteresis.

Relaxation times t_r about this stationary state are estimated by $(g^G_{,G})^{-1}$,[25] and are on the order of τ. This is also the relaxation time of most-probable firing rates, as calculated in Eqs. (2.9)—(2.11), and is consistent with the basic hypotheses of this development.

For changes in Z that transpire within a Δt of several tenths of a second to many seconds, e.g., during typical attention spans, hysteresis is more probable than simple jumps between minima if the following inequalities are satisfied. These estimates necessarily require more details of the system in addition to t_r and t_{vp}.[25] For example a,

$$\left|\frac{t_r\Delta t\Delta\underline{\bar{L}}_{,E}}{\Delta Z}\right|^{-1}|\bar{M}|\gg\frac{\Delta Z}{\Delta t}\gg\left|\frac{N\tau t_{vp}\Delta\underline{\bar{L}}}{\Delta Z}\right|^{-1}, \tag{3.10a}$$

which leads to

$$50\tau^{-1}\gg\frac{\Delta Z}{\Delta t}\sim10^{-4}\tau^{-1}\overset{?}{\gg}10^{-66}-3\,\tau^{-1}, \tag{3.10b}$$

where the numerical estimate has used $t_r=\tau$, $t_{vp}\sim1-10^{66}\,\tau$, $\Delta t=10^2\tau$, $\Delta Z=10^{-2}$, $|\bar{M}|=10$, and from Eq. (3.6) about the minima at (6,3) taking $\Delta Z=\Delta A^E_3$, $\tau\Delta\underline{\bar{L}}_{,E}/\Delta Z=2.28\times10^{-3}$ and $\tau\Delta\underline{\bar{L}}/\Delta Z=2.29\times10^{-3}$. $||\underline{\bar{L}}_{,GG'}||$ has been taken to be of the same order of magnitude at peaks and valleys; e.g., H only varies between 2.45×10^{-8} and 3.49×10^{-8} throughout the range of minima clustered about (0,0), although it increases to 8.04×10^{-7} at (117.85,23.57) and to 0.271 at (−124.99,−25).

Therefore, it is possible for hysteresis to be highly more probable than simple jump behavior to another firing state. This provides a mechanism whereby an extended temporal firing pattern of information can be processed beyond the time scale of relaxation periods, e.g., reverberation among several local minima. It is to be expected that the effects of $J_G(r;t)$ on $\Delta Z(r;t)$ create more complex examples of spatial-temporal hysteresis. These sustaining mechanisms may serve to permit other biochemical processes to store information for longer time periods as stable synaptic modifications, discussed subsequently.

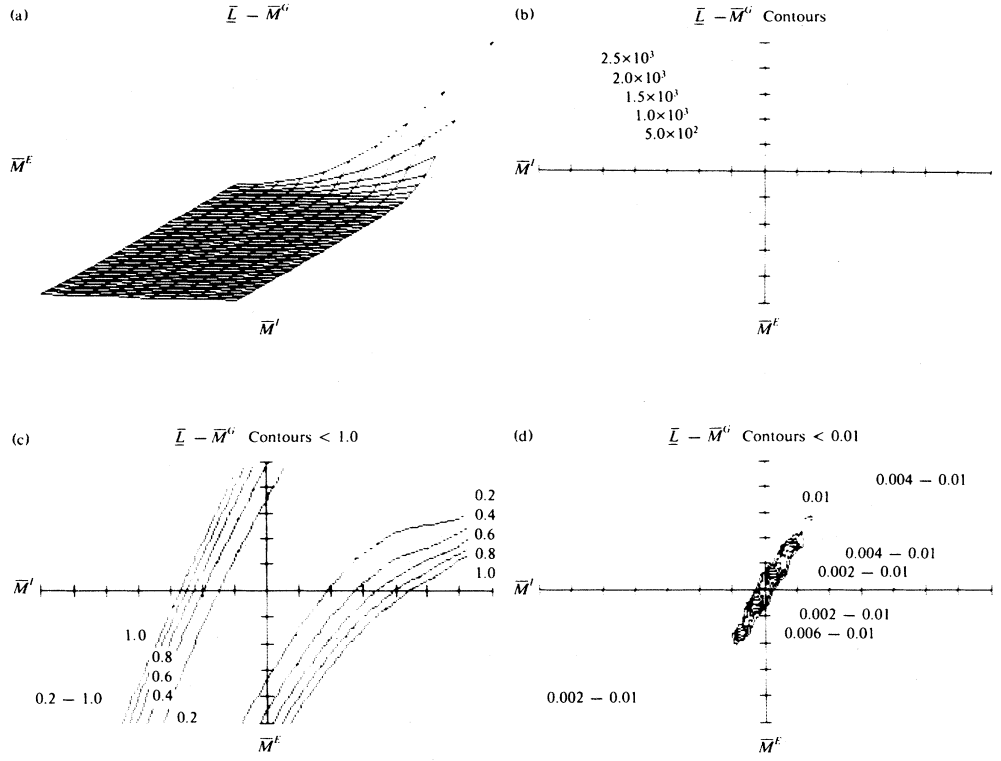

FIG. 5. In (a) the stationary Lagrangian, $\bar{\underline{L}}$, for example a is plotted versus $\bar{M}^G$. Axes and perspective are as described in Fig. 2. (b) gives a contour plot of $\bar{\underline{L}}$. (c) gives the contour plot for $\tau\bar{\underline{L}} \leq 1.0$. (d) gives the contour plot for $\tau\bar{\underline{L}} \leq 0.01$, where labels give ranges from low to high contours for 6 minima. The single closed contour about 0.01 is essentially a plateau, not to be considered a minimum. The global seventh minimum is at (0,0).

As calculated in Eq. (3.10a), it is interesting that neocortex possesses intrinsic parameters and extrinsic driving forces that make hysteresis sometimes highly improbable as well as other times highly probable, i.e., the second inequality in Eq. (3.10b) is not always satisfied. With respect to this flexibility, neocortex is quite unusual.[25]

D. Shifts in synaptic modifications

It is important to examine how spatial-temporal shifts in synaptic modifications may be stabilized for long time periods, i.e., to increase[52] as well as decrease efficacies. For instance, consider keeping fixed $\langle\langle M^G\rangle\rangle = 0$ for example B, e.g., by extrinsic $J_E = 1.33$ and $J_I = -1.19$ [cf. constraints on example b1 in Eq. (2.13)], and observe shifts in $\underline{L}_F$ associated with changes in A^G, e.g., ΔA_2^G. Expanding in powers of ΔA_2^G, to second order in $\bar{\underline{L}}_F$ to gauge the stability of A_2^G with respect to $\langle\langle \bar{M}^G\rangle\rangle$, and to first order in the differential contributions to gauge effects on spatial-temporal interactions, obtain the modifications $\Delta\underline{L}_F$ from Eq. (3.5) to $\underline{L}_F$:

$$\begin{aligned}\tau\Delta\underline{L}_F \simeq & -0.774\Delta A_2^E + 0.0989\Delta A_2^I + 2.27(\Delta A_2^E)^2 - 4.13\times10^{-4}\Delta A_2^E\Delta A_2^I + 0.204(\Delta A_2^I)^2 \\ & + (-3.95\times10^{-3}\Delta A_2^E + 1.36\times10^{-4}\Delta A_2^I)(\nabla\underline{M}^E)^2 + (-2.77\times10^{-3}\Delta A_2^E + 1.76\times10^{-4}\Delta A_2^I)(\nabla\underline{M}^I)^2 \\ & - 4.90\times10^{-5}\Delta A_2^E(\dot{\underline{M}}^E)^2 + 1.63\times10^{-4}\Delta A_2^I(\dot{\underline{M}}^I)^2 - (0.0176\Delta A_2^E - 1.15\times10^{-4}\Delta A_2^I)\dot{\underline{M}}^E \\ & - (0.0125\Delta A_2^I + 8.62\times10^{-5}\Delta A_2^E)\dot{\underline{M}}^I . \end{aligned} \tag{3.11}$$

This calculation demonstrates how the stability of synaptic modifications and associated columnar interactions may be statistically maintained during the codification and sustenance of a given firing pattern. E.g., a stable pattern is possible for $\Delta A_2^I = 7.82\Delta A_2^E$, since the remaining coefficients of the $(\Delta A_2^G)^2$ terms are positive for this example.

Most likely, synaptic modifications, hysteresis,

mesocolumnar interactions, shifts in firing patterns, long-ranged couplings, and constraints from external stimuli are highly interactive phenomena *in vivo*. Indeed, all these aspects are relevant in Eqs. (3.7), (3.10a) and (3.11).

Any definitive calculation of the dynamics of macroscopic regions of neocortex must include spatial-temporal effects in $\underline{L}_F$ from M^G, ∇M^G, and J_G. A Monte Carlo program has been formulated to directly calculate $\tilde{P}[\tilde{M}(t)]$ from the path integral in Eq. (2.5) using the prepoint discretization defined by $\underline{L}$. An importance-sampling algorithm is used,[56] extended to weight arbitrary paths according to $\exp(-N\tau\underline{L})$ and to accumulate probabilities of finding M^G in $(M^E,M^I;x,y;t')$ space. Each accumulated probability is weighted by the measure $g^{1/2}[M^E(r;t'),M^I(r;t')]$, and afterwards normalized by summing over all $(r;t')$ points sampled, $\sum P=1$. By also accumulating probabilities within several large t' bins, $\{t_B\}$, $\tilde{P}(M^E,M^I;x,y;t_B)$ can be reasonably estimated at several intermediate subdivisions of t. The error in disregarding appropriate periodic boundary conditions for intermediate t_B is probably on the order of $n_B^{-1/2}$. Increments of M^G are thinned as the number of t' iterations increase, making for an efficient algorithm.

For instance, for example A, for one mesocolumn at an arbitrary (x,y) point, thereby neglecting ∇M^G spatial interactions but including M^G temporal interactions, the probability distribution $P[M(t)]$ of M_s^G at macroscopic times was calculated, at 25τ, 50τ, 100τ, 200τ, and 300τ. Table II gives the means $\langle M^G\rangle=\sum M^G P$, the mean-square deviations $\sigma^{GG'}=[n_B^{-1}\sum(M^G-\langle M^G\rangle)(M^{G'}-\langle M^{G'}\rangle)P]^{1/2}$, and n_B = number of t' points sampling macroscopic times in bin t_B. Initial Markov paths were taken to be Gaussian distributions with means $\langle\langle\bar{M}^G\rangle\rangle$ and standard deviations $\sigma_0^{EE}=5$ and $\sigma_0^{II}=2$, but with initial time M_0^G and final times M_{100}^G and M_{300}^G set equal to $\langle\langle\bar{M}^G\rangle\rangle$. The coarse t' sampling of only 400 iterations was dictated by availability of computer resources. For the first 200 iterations, paths were incremented randomly and independently within $\Delta M^E=\pm5$ and $\Delta M^I=\pm2$, and tested for chance increases in $\exp(-N\tau\underline{L})$ to identify most important contributors which were then accrued in $P(M^E,M^I;t_B)$ bins. The last 200 iterations set $\Delta M^E=\Delta M^I=\pm1$. Probabilities were collected within bins of integer $-N^G\leq M^G\leq N^G$, within bins of t_B. For example, for the second set of calculations in Table II, values of M^G actually selected to populate the largest bin ranged from $-12\leq M^E\leq13$ and $-6\leq M^I\leq4$, sufficient to span the local minima clustered about (1.90,0.939). One set of values at 100τ was calculated as an end point in the first set of three values, and another set as a subdivision of the next set of three values. The difference of these two sets of values is due primarily to the small number of iterations. However, the first set of values does demonstrate that for example a the system remains stable in its relaxed state, and the calculation of the evolution of means and mean-square deviations of M^G demonstrates how $\langle M^G\rangle$ is shifted due to $\bar{M}^G$ influences and fluctuation among other local minima. This formalism does not warrant calculating a path integral for small time scales, e.g., less than 25τ.

E. Future studies

(a) Other applications of this formalism using the the Stratonovich paradigm will require using $\underline{L}_F$ in Eq. (2.7), instead of $\underline{L}$ in Eq. (2.5), making it necessary to do further numerical studies of $\underline{L}_F$, despite two orders of magnitude increased algebraic complexity. Note that the Riemannian terms $\underline{V}-\underline{V}'$ given in Table I illustrate that these give a measurable contribution to $\underline{L}_F$.

(b) Future calculations will add spatial $\nabla\tilde{M}$ interactions and spatial-temporal $J_G(r;t')$ to study the evolution of evoked potentials, and their effects on synaptic modifications $\Delta Z(r;t)$. The GL expansions calculated in Sec. II C can be utilized to investigate long-time and long-ranged order in the evoked regions, e.g., roll or polygon patterns.

(c) The previous Monte Carlo calculation also permits inclusion of effects of interactions at $(r;t')$ in a given lamina, labeled by λ, from other statistically independent laminae at point r and nearest-neighbor r' points at time $t-\tau$. Along with the inclusion of interlaminar circuitry, the definition of a mesocolumn can be extended to include interminicolumnar efferent circuitry, by including higher order NN's as mentioned in Sec. II B.

TABLE II. At two macroscopic times t_B, 100τ and 300τ, each sample with three subdivisions of n_B points, a Monte Carlo calculation of the path integral for example a yields the means $\langle M^G\rangle$ and mean-square deviations $\sigma^{GG'}$. Differences at 100τ and nonzero σ^{EI} are due primarily to the small number of points sampled.

t_B/τ	n_B	$\langle M^E\rangle$	σ^{EE}	$\langle M^I\rangle$	σ^{II}	σ^{EI}
25	96	−1.50	3.40	−1.22	1.55	1.31
50	202	−1.58	2.41	−1.28	1.10	0.730
100	400	−1.60	1.68	−0.929	0.825	0.476
100	129	−1.05	3.33	−0.928	1.39	0.781
200	273	−1.19	2.28	−1.24	1.03	0.623
300	400	−1.49	1.83	−1.11	0.831	0.552

For example, to address interlaminar circuitry, using the prepoint discretization of Eq. (2.2), replace $G \to \lambda G$ and let $\lambda = 1, \ldots, 6$. A reasonable description has the predominantly middle and upper laminas driven by $J_{\lambda G}$, e.g., to account for thalamocortical and inter-regional processes. The predominantly lower efferent laminas and higher afferent laminas are described by $\{\alpha^{\lambda G}, \beta^{\lambda G}, \gamma^{\lambda G}\}$ in modified Eq. (2.4), determined from $\{A^{*\lambda G}, B^{*\lambda G}, v^{\lambda G}, \phi^{\lambda G}, N^{*\lambda G}\}$ which are obtained from $\sum_{k \in \lambda'}$ in Eq. (2.1). These effects accumulate to cause firing transitions from $M^{\lambda' G'}(r';t')$ to $M^{\lambda G}(r;t'+\tau)$, where λ is an internal index summed over in $\underline{L} = \sum_{\lambda G} \underline{L}^{\lambda G}$ similar to the sum over G in the absence of the λ indices. For example,

$$\sum_{k \in \lambda'} a^*_{j_\lambda k} v^2_{j_\lambda k} \to (v^{\lambda\lambda' G})^2 (N^{\lambda' G} a^{\lambda\lambda' G} + \tfrac{1}{2} A^{\lambda\lambda' G} M^{\lambda' G}) \, , \tag{3.12}$$

$$\theta \dot{M}^G(t') \to \theta \dot{M}^{\lambda G}(t') = M^{\lambda G}(t'+\theta) - M^{\lambda G}(t') \, .$$

The readily derived result is a probability distribution highly nonlinear in λ. This permits explicit inclusion of ongoing alterations in synaptic parameters: For a given path chosen as described previously, changes in $\underline{L}^\lambda$ in lamina λ at location r at time $t'+\tau$ are determined by changes in $J_{\lambda G}$ and ΔZ transpiring at time t' from laminas λ' at locations $r \leq r \pm \rho$. These ΔZ modifications may in turn be due to changes in $J_{\lambda G}$ and/or to changes in firings $M^{\lambda G}$ necessary to encode and process patterns of firings $\langle \langle M^{\lambda G} \rangle \rangle$.

Interactions between two or more macroscopic regions, denoted by indices Λ, arising from long-ranged fibers, may be modeled by $\underline{L}_F = \sum_\Lambda \underline{L}^\Lambda_F$ by adding to $\underline{L}^\Lambda_F$

$$\underline{J}_{\Lambda\lambda G}(r^\Lambda;t') M^{\Lambda\lambda G}(r^\Lambda;t') = C_{\Lambda\Lambda'\lambda\lambda' GG'} M^{\Lambda'\lambda' G'}(\bar{r}^{\Lambda'};t'-t_{\Lambda\Lambda'}-\tau) M^{\Lambda\lambda G}(r^\Lambda;t') \, , \tag{3.13}$$

where $t_{\Lambda\Lambda'}$ is the time of transmission from Λ' to Λ, which can be on the order of 10–30 msec, $C_{\Lambda\Lambda'\lambda\lambda' GG'}$ are empirically fitted couplings between firings in regions Λ and previous spatially averaged firings in region Λ', and GG' is predominantly EE. The spatial averaging in region Λ', denoted by $\bar{r}^{\Lambda'}$, is not required, but is suggested for reasonable first order computer calculations.

(d) There is some empirical evidence to support the conjecture of chaotic behavior[36,57,58] in neocortex, driven by changes in concentrations of neurotransmitters.[59] The observed time scale of this phenomenon is hundreds of seconds, but no metric or measure space yet has been established to analytically explain the empirical evidence. It is reasonable to assume that these chemical changes effect synaptic changes, e.g., in $\Delta A^G(r;t')$ and $\Delta B^G(r;t')$, which drive neuronal firing states. This may induce chaotic behavior in firing states, and/or particular firing patterns may be an essential component of a mechanism causing chaotic behavior of the chemical product accumulation rates. E.g., under some conditions, the "information dimension" measuring the space mapped out by the probability distribution of $M^G(r;t')$ may be a noninteger less than the initial phase space dimension, essentially $2[dM_0^{Gv}]$ in Eq. (2.5). There is good evidence that the measure of this information dimension can be calculated efficiently from the Lyapunov dimension, which measures the (in)stability of $M^G(r;t')$ trajectories; chaos results if at least one Lyapunov exponent > 0.[57] A direction for future study of these phenomena examines the evolution of the conditional probabilities of mesocolumnar firings as given by the previous path integral. A relatively simple function for first study of this stochastic evolving map on $M^G(r;t_0)$ is given by the prepoint-discretized Lagrangian $\underline{L}$ expanded to first order in the external driving parameter ΔA^G or ΔB^G, as in Eq. (3.6).

Chaotic behavior of mesocolumns induced by long-ranged constraints J_G may account for observed intermittent bursting of firing patterns on time scales of tenths of a second. Synchronized bursting of mesocolumnar firings is also a candidate for explaining information processing, in addition to stochastic processing and reverberation among local minima of firing patterns. For example, changing J_G drives $\underline{L}_F$ to various local minima, giving rise to various evolving $\underline{L}$ or $\hat{H}$ stochastic maps, some of which can lead to chaotic behavior, similar to that observed for the logistic map, via the route of intermittency.[60]

(e) As more detailed neuronal parameters become available, more detailed renormalization-group studies of regional activity can profitably utilize GL polynomials, demonstrated in Sec. II C to be valid expansions about stationary firing minima, to study phase transitions. The expansion coefficients of GL polynomials of $\underline{L}$ are expected to be measurably renormalized by multiple scales of fluctuations present between mesoscopic and macroscopic scales. Fluctuations present between microscopic and mesoscopic scales presumably have been included in developing the mesoscopic scale. For example, these studies are also necessary for definitive analyses of the previous future projects (b) and (d).

(f) Beyond their classical interactions across several spatial-temporal scales, spanning membrane to regional activities as presented here, under some conditions of cooperation and competition among

these multiple hierarchies, there may exist sensitive interactions between macroscopic regional scales and quantum synaptic or membrane scales. Critical points, of cooperative behavior or diverging chaotic trajectories defined at a given scale, essentially may reflect sensitivity to initial conditions and interactions at smaller scales. For example, as noted previously, these critical points may plausibly exist at the following: membrane scales—phase transitions among gated synaptic and membrane activities[12,53]; mesoscopic scales—chaotic behavior or second-order phase transitions of columnar firing states; and macroscopic scales—chaotic behavior of neurotransmitters or wave propagation. Competition at a given scale, causing large cancellations among interactions, also enhances sensitivity to smaller scales. For example, as noted previously, these cancellations occur at the following: membrane scales—at ionic and neurotransmitter gates; microscopic scales—E and I competition among many synapses; and mesoscopic scales—NN minicolumnar interactions from neighboring macrocolumnar domains.

Hypotheses of decision-making and problem-solving based on interactions between relatively small and large scales,[61,62] may require interactions at critical points of chaotic or phase transitions of mesoscopic $M^G(r;t)$ trajectories.[45] For example, a wave function or packet involving synaptic and membrane interactions over regional scales may represent alternative future macroscopic events by branching into distinct wave functions,[63] the absolute square of each being a statistical measure associated with a specific $\tilde{P}(\tilde{M})$.[64] At these critical points, reflecting microscopic sensitivity to these quantum alternatives, mesoscopic processing, and stored information structures—represented by $\tilde{L}$, neuronal parameters $\{\alpha^G,\beta^G,\gamma^G\}$, and initial conditions $\tilde{P}[\tilde{M}(0)]$—"recognize" (or reduce) one of these alternative quantum wave functions, thereby necessitating a true freedom of choice or even creation of a macroscopic firing pattern. This also may generate macroscopic nonlocal interactions of information associated with the other branching wave functions. Empirical verification of these events would have important implications for current unresolved issues in the foundations of quantum theory and the mind-body problem.[65,66] Note that a "weakened" stochastic choice of a firing pattern is still operative at macroscopic scales due to the evolution and interaction of nonlinear nonequilibrium probability distributions of alternative $\tilde{M}$ trajectories: This stochasticity arises from statistically averaging over microscopic and membrane scales which represent chemical-electrical processes transpiring at quantum scales, but not necessarily from statistical correlations induced by the process of macroscopic measurement of quantum interactions.

IV. DISCUSSION

Detailed calculations have been presented to support a scenario of neocortical columnar coding of extrinsic stimuli, short-term storage via hysteresis, and long-term storage via synaptic modification. This development has assumed that, at the synaptic interaction scale of 10^{-2} μm, neocortical information is statistically processed primarily by voltage-gated presynaptic and chemically gated postsynaptic interactions. Among a collection of hundreds of neurons, mesocolumns encompassing one to several minicolumns on a scale of 10^2 μm communicate via $\sim 10^6$ synaptic interactions. Long-ranged fibers contribute driving forces on these rates of firings of short-ranged fibers.

This description of neocortical interactions, although correctly viewed for purposes of single neuronal studies as a gross simplification of complex microscopic details of neocortex, is reasonable and appropriate to investigate macroscopic properties of neocortex. In the literature, there are many theoretical treatments of neocortical phenomena based on averaged neuronal interactions and random noisy backgrounds. These basic assumptions must be analyzed with the same scrutiny given to the empirical data and to mechanisms proposed for their explanation. In this development much empirical neuronal information is explicitly retained without adding any undefined or unphysical parameters, and the net formalism falls within the scope of modern treatments of collective systems. A direction is specified for correcting previous modeling of neocortex that includes the salient features of this development. Some tentative conjectures on neocortical and neuropsychological mechanisms have been made elsewhere.[1,45,61] This approach to understanding properties of macroscopic neocortex offers a reasonable balance between two realistic constraints: to include as much microscopic neuronal detail as possible without requiring unreasonable computer calculations of the mesoscopic columnar system.

Although experimental uncertainty prohibits giving definitiveness to any particular set of neuronal parameters, within the empirical range of these sets, several macroscopic properties of neocortex have been analyzed, giving insight into information processing of real brains and into some features desired in artificial (computer) intelligence. It is now possible to explicitly calculate spatial-temporal firing pat-

terns of columns, as demonstrated by a Monte Carlo program. The dynamics of synaptic modification demand that their nonlinear interactions with these most probable firing patterns be explicitly accounted for in any treatment of information processing or storage. This has been demonstrated by calculating changes and stabilities of most probable firing patterns associated with changes of electrical-chemical presynaptic and postsynaptic parameters induced by extrinsic sources, and by calculating the probability of extrinsic sources enabling hysteresis of firing patterns to retain information for epochs longer than typical relaxation periods. Explicit directions are given for future study of interlaminar and interregional interactions and chaotic behavior.

ACKNOWLEDGMENTS

Algebraic calculations were facilitated with the PDP-10 MACSYMA Consortium algebraic manipulator at Massachusetts Institute of Technology, supported in part by U.S. ERDA E(11-1)-3070 and NASA NSG 1323. Numerical calculations were facilitated with the VAX and text preparation was facilitated with the PDP-11/70 CATT systems at the University of California at San Diego. This project has been supported entirely by personal contributions to Physical Studies Institute and to the University of California at San Diego Physical Studies Institute agency account through the Institute for Pure and Applied Physical Sciences.

[1]L. Ingber, Physica 5D, 83 (1982).
[2]M. Büttiker and H. Thomas, Phys. Rev. A 24, 2635 (1981).
[3]H. Haken, *Synergetics,* 2nd ed. (Springer, New York, 1978).
[4]S.-K. Ma, *Modern Theory of Critical Phenomena* (Benjamin/Cummings, Reading, Mass., 1976).
[5]G.F. Mazenko, M.J. Nolan, and O.T. Valls, Phys. Rev. B 22, 1275 (1980).
[6]V.B. Mountcastle, in *The Mindful Brain,* edited by G.M. Edelman and V.B. Mountcastle (Massachusetts Institute of Technology, Cambridge, 1978), p. 7.
[7]E.R. John and E.L. Schwartz, Annu. Rev. Psychol. 29, 1 (1978).
[8]R. Näätanen, Biol. Psych. 2, 237 (1975).
[9]P.L. Nunez, *Electric Fields of the Brain: The Neurophysics of EEG* (Oxford University Press, New York, 1981).
[10]S.J. Williamson, L. Kaufman, and D. Brenner, J. Appl. Phys. 50, 2418 (1979).
[11]V. Hamburger and R.W. Oppenheim, Neurosci. Commen. 1, 39 (1982).
[12]I. von der Heydt, N. von der Heydt, and G.M. Obermair, Z. Phys. B 41, 153 (1981).
[13]D.A. Pink, A. Georgallas, and M.J. Zuckermann, Z. Phys. B 40, 103 (1980).
[14]F.O. Schmitt, P. Dev, and B.H. Smith, Science 193, 114 (1976).
[15]C.P. Taylor and F.E. Dudek, Science 218, 810 (1982).
[16]M. Abeles, *Local Cortical Circuits* (Springer, New York, 1982).
[17]H. Korn, A. Triller, A. Mallet, and D.S. Faber, Science 213, 898 (1981).
[18]G.M. Shepherd, *The Synaptic Organization of the Brain,* 2nd ed. (Oxford University Press, New York, 1979).
[19]J. Mathews and R.L. Walker, *Mathematical Methods of Physics,* 2nd ed. (Benjamin, New York, 1970).
[20]A.K. Afifi and R.A. Bergman, *Basic Neuroscience* (Urban & Schwarzenberg, Baltimore, 1978).
[21]R.W. Dykes, Prog. Neurobiol. 10, 33 (1978).
[22]V. Braitenberg, in *Architectonics of the Cerebral Cortex,* edited by M.A.B. Brazier and H. Petsche (Raven, New York, 1978), p. 443.
[23]E.L. Bienenstock, L.N. Cooper, and P.W. Munro, J. Neurosci. 2, 32 (1982).
[24]Ch. von der Malsburg, Biol. Cybernetics 32, 49 (1979).
[25]G.S. Agarwal and S.R. Shenoy, Phys. Rev. A 23, 2719 (1981).
[26]L. Sneddon, Phys. Rev. A 24, 1629 (1981).
[27]D. Walgraef, G. Dewel, and P. Borckmans, Z. Phys. B 48, 167 (1982).
[28]F. Langouche, D. Roekaerts, and E. Tirapegui, Nuovo Cimento 53B, 135 (1979).
[29]F. Langouche, D. Roekaerts, and E. Tirapegui, J. Phys. A 13, 449 (1980).
[30]R. Graham, in *Stochastic Processes in Nonequilibrium Systems,* edited by L. Garrido, P. Seglar, and P.J. Shepherd (Springer, New York, 1978), p. 82.
[31]H. Dekker, Physica 103A, 586 (1980).
[32]B.S. DeWitt, Rev. Mod. Phys. 29, 377 (1957).
[33]W.J. Freeman, *Mass Action in the Nervous System* (Academic, New York, 1975).
[34]H.R. Wilson and J.D. Cowan, Biophys. J. 12, 1 (1972).
[35]N.G. van Kampen, *Stochastic Processes in Physics and Chemistry* (Elsevier, New York, 1981).
[36]H. Haken and G. Mayer-Kress, Z. Phys. B 43, 185 (1981).
[37]H. Dekker, Phys. Lett. 80A, 99 (1980).
[38]K.A. Fitzpatrick and T.J. Imig, J. Comp. Neurol. 192, 589 (1980).
[39]P.S. Goldman and W.J.H. Nauta, Brain Res. 122, 393 (1977).
[40]D.H. Hubel and T.N. Wiesel, J. Physiol. 160, 106 (1962).
[41]D.H. Hubel and T.N. Wiesel, Proc. R. Soc. London, Ser. B 198, 1 (1977).

[42]E.G. Jones, J.D. Coulter, and S.H.C. Hendry, J. Comp. Neurol. 181, 291 (1978).
[43]E.R. Kandel and J.H. Schwartz, *Principles of Neural Science* (Elsevier, New York, 1981).
[44]P. Rakic, Science 214, 928 (1981).
[45]L. Ingber, J. Social Biol. Struct. 4, 211 (1981).
[46]R.M. Shiffrin and W. Schneider, Psych. Rev. 84, 127 (1977).
[47]V.B. Mountcastle, R.A. Andersen, and B.C. Motter, J. Neurosci. 1, 1218 (1981).
[48]J.A. Anderson, J.W. Silverstein, S.A. Ritz, and R.S. Jones, Psych. Rev. 84, 413 (1977).
[49]J. Hérault, G. Bouvier, and A. Chehikian, J. Phys. (Paris) Lett. 41, 75 (1980).
[50]S. Marčelja, J. Opt. Soc. Am. 70, 1297 (1980).
[51]L. Ingber, Phys. Rev. 174, 1250 (1968).
[52]D.O. Hebb, *The Organisation of Behavior* (Wiley, New York, 1949).
[53]J.F. Nagle, Annu. Rev. Phys. Chem. 31, 157 (1980).
[54]E.R. Kandel and J.H. Schwartz, Science 218, 433 (1982).
[55]H.R. Wilson, Vision Res. 17, 843 (1977).
[56]S.V. Lawande, C.A. Jensen, and H.L. Sahlin, J. Comput. Phys. 3, 416 (1969).
[57]J.D. Farmer, Physica 4D, 366 (1982).
[58]E. Ott, Rev. Mod. Phys. 53, 655 (1981).
[59]A. Mandell and P.V. Russo, J. Neurosci. 1, 380 (1981).
[60]J.E. Hirsch, B.A. Huberman, and D.J. Scalapino, Phys. Rev. A 25, 519 (1982).
[61]L. Ingber, J. Social Biol. Struct. 4, 225 (1981).
[62]L. Ingber, *Karate: Kinematics and Dynamics* (Unique, Hollywood, 1981).
[63]H. Everett, III, in *The Many-Worlds Interpretation of Quantum Mechanics,* edited by B.S. DeWitt and N. Graham (Princeton University Press, Princeton, 1973), p. 3.
[64]A.A. Broyles, Phys. Rev. D 25, 3230 (1982).
[65]H.P. Stapp, Found. Phys. 12, 363 (1982).
[66]H.P. Stapp, Lawrence Berkeley Laboratory Report No. LBL-15363, 1982 (unpublished).